energies

Review

Sea Wave Energy. A Review of the Current Technologies and Perspectives

Domenico Curto *, Vincenzo Franzitta and Andrea Guercio

Department of Engineering, University of Palermo, 90128 Palermo, Italy; vincenzo.franzitta@unipa.it (V.F.); andrea.guercio@unipa.it (A.G.)
* Correspondence: domenico.curto@unipa.it

Abstract: The proposal of new technologies capable of producing electrical energy from renewable sources has driven research into seas and oceans. Research finds this field very promising in the future of renewable energies, especially in areas where there are specific climatic and morphological characteristics to exploit large amounts of energy from the sea. In general, this kind of energy is referred to as six energy resources: waves, tidal range, tidal current, ocean current, ocean thermal energy conversion, and saline gradient. This review has the aim to list several wave-energy converter power plants and to analyze their years of operation. In this way, a focus is created to understand how many wave-energy converter plants work on average and whether it is indeed an established technology.

Keywords: sea wave; WEC; point absorber; terminator; attenuator; OWC; WAB; OD

Citation: Curto, D.; Franzitta, V.; Guercio, A. Sea Wave Energy. A Review of the Current Technologies and Perspectives. *Energies* **2021**, *14*, 6604. https://doi.org/10.3390/en14206604

Academic Editor: Elisabetta Tedeschi

Received: 31 August 2021
Accepted: 9 October 2021
Published: 13 October 2021

1. Introduction

This review is focused on the exploitation of sea wave energy. However, this is just one of the several kinds of energy, related to the oceanic environment, thus a brief description of the main sea energy resources is necessary [1,2].

Oceans represent an enormous energy reserve that is distributed in different phenomena. Among these, the main kinds of energies related to the oceans are marine currents, osmotic salinity, OTEC (acronym of Ocean Thermal Energy Conversion), tide, and sea wave.

Each oceanic energy source has a relevant potential for human applications; however, as shown in Table 1, sea waves and marine currents have the highest energy potentials [3].

Table 1. Potential installable capacity and energy production from marine energy sources [3].

Ocean Energy	Capacity (GW)	Potential Generation (TWh/y)
Tide	90	800
Marine currents	5000	50,000
Osmotic salinity	20	2000
OTEC	1000	10,000
Sea wave	1000–9000	8000–80,000

All these oceanic energy sources are classified as renewable [4]. Indeed, tides are due to the Moon's orbit around the Earth, the orbit of this one around the sun, and the Earth's rotation. As consequence, a huge amount of seawater flows around the world's surface, modifying locally the sea level. The effects are locally different due to the irregular distribution of lands around the world. In any case, the tides are a regular phenomenon, whose effects can be accurately predicted. Thus, tides represent an interesting renewable energy source, allowing the exploitation of tidal streams or tidal ranges. The second one has few applications worldwide, since this phenomenon allows the installation of

the power plant close to the coastline, realizing a barrier equipped with low-head hydro turbines. The first one was the power plant in La Rance (France), installed in 1966 and still operating. Other plants are installed in Russia (Kislaya Guba, 1.7 MW), Canada (Annapolis Royal Generation Station, 20 MW), China (Jiangxia, 3.9 MW), and Korea (Lake Sihwa. 254 MW) [5].

The term ocean current is used to underline the different origin of marine currents in comparison to the tidal currents, previously described. Ocean currents are seawater circulations promoted by solar energy. Since the solar radiation varies with the latitude and considering the irregular distribution of the lands on the Earth's surface and the orography of seabed, the variation of water density produces water flows that are extended for thousands of kilometers. Superficial currents are, also, created by the wind interactions (that is also an effect of solar radiation) with the sea surface. Summing all these contributions, the thermohaline circulation is generated. The Gulf Stream is a famous ocean current (about 100 km wide and 800 m to 1200 m deep) that is originated from the Gulf of Mexico and flows up the North Pole with a speed of about 2.5 m/s [6]. Other famous currents are the Kuroshio Current (on the west side of Pacific Oceans) [7] and the Agulhas Current (on the south-eastern part of the Indian Ocean, along the coastline of South Africa) [8].

About the Ocean Thermal Energy Conversion (OTEC), the idea is the installation of a thermal machine using the superficial seawater as a thermal source and the deep water as a thermal sink [9]. The main problem is the low energy efficiency of this system, also in the best cases. Considering the installation of an ideal Carnot heat engine to exploit the available thermal sources, the energy efficiency is no more than 7%. Consequently, introducing the irreversibility of a real system, the power plant requires huge dimensions (especially the heat exchangers) to obtain a significant power output; thence the required investments are high. Two layouts for a possible OTEC power plant have been proposed: open cycle and closed cycle [9,10]. In the first one, the warm water from the sea surface is flashed to produce steam and then condensed using the cold deep water. The main disadvantages are related to the operative conditions. Indeed, steam generation requires a vacuum condition along with the entire plant, so air infiltration is possible. At the same time, the specific mass of steam is quite high (30–100 m^3/kg), hence the system requires large pipes for small power outputs. In the second solution, the warm superficial water is used to evaporate a working fluid, normally used in the chilling sector such as ammonia, propane, or chlorofluorocarbon. This vapor is used to run a turbine, then it is condensed using the deep water as a refrigerant. The advantage is that the system works under pressure, so air infiltration is avoided. As a disadvantage, large heat exchangers are required [11].

About the saline gradient energy source (called also Osmotic Power), the idea is the exploitation of chemical energy released when the freshwater from rivers is mixed with saltwater in the sea. Two solutions with different ions concentrations are characterized by different values of osmotic pressure. A solution, proposed in 1937, is the Pressure Retarded Osmosis, where the saltwater is pressurized before a semipermeable membrane. If the external pressure gradient is lower than the osmotic pressure, water flows from the diluted solution to the concentrated one. Brackish water is consequently produced, with the same pressure as the saline water but with a greater flow. Using a hydro turbine is possible to collect more energy than the pumping expenditure, producing an electrical output [12,13].

Finally, sea wave is a form of marine energy due to the several forces acting on the water surface, such as the friction generated by wind, the Coriolis force (related to the Earth rotation), the celestial bodies attraction (tidal), or other unpredictable phenomena as earthquake and volcanic eruptions (tsunami) [14]. In any case, to describe this energy source, some definitions are required.

2. Definitions

A regular wave is classically modelled by a sine (or cosine) function of time and position, introducing the amplitude A, the wavelength λ, and the period T, reported in Equation (1) [15].

$$z_w(x,t) = A\,sin\left(\frac{2\pi}{T}t - \frac{2\pi}{\lambda}x\right) \tag{1}$$

In detail, fixing the observing time t_0, the wavelength λ represents the minimal distance over which the wave shape is repeated, as shown in Figure 1.

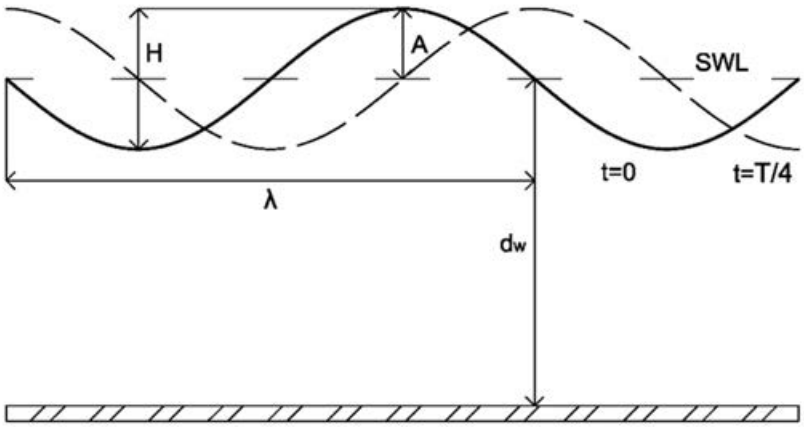

Figure 1. Parameters for a regular wave.

Similarly, selecting the observing point x_0, the period T represents the minimal time required to complete a single oscillation. Both conditions are expressed by the relations reported in Equation (2), considering n as a generic natural number [15].

$$\begin{aligned} z_w(x + n\lambda, t_0) &= z_w(x, t_0) \\ z_w(x_0, t + nT) &= z_w(x_0, t) \end{aligned} \tag{2}$$

The rate of propagation (called also phase velocity) v_p represents the speed at which the wave profile travels and is given by the ratio λ/T.

The amplitude A represents the measure of the entire oscillating phenomenon in a single period. Two definitions are commonly used:

- Peak amplitude, i.e., the difference between the peak and the Surface Water Level (SWL). This definition is commonly used in the electronics sector.
- Peak-to-peak, i.e., the difference between the crest (the highest value during the oscillation) to the trough (the lowest one).

To avoid misunderstanding, in the sea wave sector the term "height" (symbol H) is normally used to indicate the peak-to-peak amplitude (see Figure 1).

Equation (1) can be used also to introduce other two parameters. The amount $2\pi/T$ is called angular frequency and is indicated with the Greek letter ω. Similarly, the amount $2\pi/\lambda$ is the wavenumber and indicated with k. Finally, the steepness is a nondimensional number given by the ratio H/λ.

The parameters above introduced are commonly used to analyze the periodic signal, also irregular, by introducing the Fourier series. Considering only a time-dependent function to simplify, a generic period signal can be approximated by Equation (3), where A_0 is the average value of the signal, $A_{s,i}$ and $A_{c,i}$ the amplitude of the harmonics used to approximate the input signal [15].

$$z_w(t) = A_0 + \sum_{i=1}^{n} A_{s,i}\,sin\left(\frac{2\pi i}{T}t\right) + \sum_{i=1}^{n} A_{c,i}\,cos\left(\frac{2\pi i}{T}t\right) \tag{3}$$

The motion of a single particle of fluid during sea motion was described by the Airy wave equations (published by Sir George Biddel Airy in 1845), representing a linear solution to the hydrodynamic equations.

$$\begin{array}{c} \Delta x = -\frac{H\ cosh\ k(z_0+d_w)}{2\ sinh\ kd_w} cos(kx_0 - \omega t - \phi) \\ \Delta z = \frac{H\ sinh\ k(z_0+d_w)}{2\ sinh\ kd_w} sin(kx_0 - \omega t - \phi) \end{array} \quad (4)$$

The particle describes an elliptical motion around the mean position (x_0, z_0) according to Equation (4) [16], tending to be circular in the surface $(z_0 = 0)$ and practically horizontal near seabed $(z_0 = -d_w)$, as depicted in Figure 2.

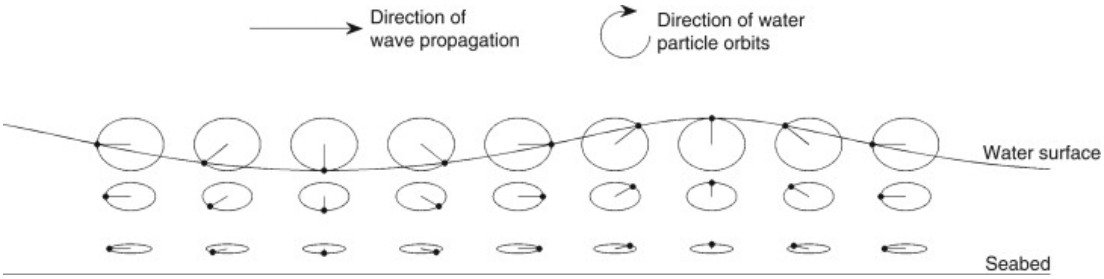

Figure 2. Particle motion in sea wave (Reproduced with permission 5139240948876 from [17], Elsevier, 2012).

Indeed, if the quote z_0 tends to $-d_w$ (seabed), the factor $cosh\ k(z_0 + d_w)$ is equal to 1 while $sinh\ k(z_0 + d_w)$ is equal to 0.

If the water depth d_w tends to ∞, Equation (4) can be simplified in Equation (5), corresponding to the case of a circular motion [14].

$$\begin{array}{c} \Delta x = -\frac{H}{2} e^{kz_0}\ cos(kx_0 - \omega t - \phi) \\ \Delta z = \frac{H}{2} e^{kz_0}\ sin(kx_0 - \omega t - \phi) \end{array} \quad (5)$$

However, the sea wave phenomenon is an example of random waves, thence a statistical approach is normally used. The following definitions are commonly adopted during a measuring campaign in the open sea. The classical approach considers the sea wave phenomenon as a sum of a large number of sine wave components, each one with different amplitude A_i, period T_i, wavelength λ_i, and direction ϑ_i [17]. The term ϕ_i represents the wave phase, considered randomly distributed in the interval $[0,\ 2\pi]$.

$$z_w(x, y, t) = \sum_{i=1}^{n} A_i\ sin\left[\frac{2\pi}{\lambda_i}(x\ cos\ \vartheta_i + y\ sin\ \vartheta_i) - \frac{2\pi}{T_i}x + \phi_i\right] \quad (6)$$

Using a statistical approach, it is possible to introduce a directional variance spectrum $s(f, \vartheta)$ indicating how the energy in the wave field is distributed with respect to frequency and direction [17].

The directional variance spectrum $s(f, \vartheta)$ can be decomposed into two functions (see Equation (7)): $s(f)$ represents the total energy at each frequency independently of wave direction, while $D(f,\ \vartheta)$ expresses how the energy at a specific frequency is distributed according to the wave direction [14].

$$s(f, \vartheta) = s(f)D(f,\ \vartheta) \quad (7)$$

By the integration over the entire space, the omnidirectional spectrum or frequency spectrum is obtained in Equation (8) [18]:

$$S(f) = \int_0^{2\pi} s(f)D(f, \vartheta)d\vartheta \quad (8)$$

where the directional distribution function $D(f, \vartheta)$ satisfies the conditions expressed by Equation (9) [14]:

$$\begin{array}{c} \int_0^{2\pi} D(f,\ \vartheta) d\theta = 1 \\ D(f,\ \vartheta) \geq 0 \ \forall \ \theta \in [0, 2\pi] \end{array} \quad (9)$$

The definition of frequency spectrum $S(f)$ is fundamental since several statistical parameters used in sea wave analysis are defined on this basis. The n-th order momentum of frequency spectrum m_n is defined by Equation (10) [18]:

$$m_n = \int_0^{\infty} f^n S(f) df \quad (10)$$

The significant height H_s is equal to four times the standard deviation of the surface elevation or equivalently as four times the square root of the zeroth-order moment of the wave spectrum [19], so:

$$H_s = 4\sqrt{m_0} = 4\sqrt{\int_0^{\infty} S(f) df} \quad (11)$$

In the past, the significant height was traditionally defined as the mean wave height of the highest third of the waves [15], according to Equation (12).

$$H_s \cong H_{1/3} = \frac{1}{n/3} \sum_{j=1}^{n/3} H_j \quad (12)$$

It is important to underline that the two definitions are practically equivalent as a more accurate correlation shows that $H_{1/3} = 4.01\sqrt{m_0}$, so the difference is negligible [19]. In the literature, sometimes other parameters are used to describe the wave height [20]:

- $H_m = H_{1/1}$ Mean wave represents the average value of all measured waves in the measuring period.
- $H_{1/10}$ Wave one-tenth is the mean wave height of the highest tenth of the waves.
- H_{max} Maximum wave height is the maximum value measured in the site. It is relevant to design structures that are exposed to sea waves.

In the literature, the average period T_m represents the average value of all waves, measured in a fixed interval (for example 30 min or 1 h). A more rigorous definition is given by Equation (13) [17]:

$$T_m = \frac{m_0}{m_1} = \frac{\int S(f) df}{\int f S(f) df} \quad (13)$$

Another common period is the mean wave period T_z defined as the square root of the zero-order momentum and the second-order momentum of the frequency spectrum (see Equation (14)) [21]:

$$T_z = \sqrt{\frac{m_0}{m_2}} = \sqrt{\frac{\int S(f) df}{\int f^2 S(f) df}} \quad (14)$$

It is also possible to define a Peak Period T_p corresponding to the peak of the variance density spectrum $S(f)$.

Finally, the wave-energy period T_e is defined as the variance-weighted mean period of the one-dimensional period variance density spectrum $S(f)$ [22]. Analytically, the energy period is defined by Equation (15):

$$T_e = \frac{m_{-1}}{m_0} = \frac{\int f^{-1} S(f) df}{\int S(f) df} \quad (15)$$

This parameter is commonly used for the evaluation of potential energy production. As Equation (15) is quite complex to perform, simplified correlations are available in the literature.

As an example, the Atlas of UK Marine Renewable Energy Resources suggests the correlation between the energy period and the average period, expressed by Equation (16) [22]:

$$T_e = 1.14\ T_p \tag{16}$$

The energy period can be also evaluated from the peak period T_p, according to Equation (17). The value 0.86 is obtained in the case of the Pierson Moskowitz spectrum [23]. This value is commonly used in the surrounded seas with a limited surface, such as the Mediterranean Sea [18].

$$T_e = 0.86\ T_m \tag{17}$$

The Pierson Moskowitz spectrum, above cited, is modelled by Equation (18), where α_{PM} e β_{PM} are two parameters related to the sea state, defined by the significant height H_s and the peak period T_p (or equivalently the peak frequency $f_p = 1/T_p$) [24,25]:

$$\begin{gathered} S_{PM}(f) = \frac{\alpha_{PM}}{f^5} e^{-\beta_{PM}/f^4} \\ \alpha_{PM} = \frac{5}{16} H_s^2 f_p^4 \beta_{PM} = \frac{5}{4} f_p^4 \end{gathered} \tag{18}$$

In the original work, the Pierson Moskowitz spectrum was related to the wind speed measured at 19.5 m above the average sea level, using a similar formulation [14].

Another common spectrum is the JONSWAP (acronym of Joint North Sea Wave Observation Project) spectrum, obtained from Pierson Moskowitz spectrum multiplied by an extra peak enhancement factor $\gamma^{\delta(f)}$ [26]:

$$\begin{gathered} S_{JONSWAP}(f) = S_{PM}(f)\gamma^{\delta(f)} \\ \delta(f) = exp\left[-\frac{1}{2}\left(\frac{f-f_p}{\sigma f_p}\right)^2\right] \\ \sigma = \begin{cases} 0.07\ for\ f < f_p \\ 0.09\ for\ f \geq f_p \end{cases} \end{gathered} \tag{19}$$

In the JONSWAP distribution, all parameters are obtained from the observed sea [17]. A qualitative comparison of the Pierson Moskovitz spectrum and JONSWAP spectrum is reported in Figure 3, where the x-axis is normalized by the peak frequency and the y-axis by the maximum value of the Pierson Moskovitz spectrum. The graph underlines the effect produced by an extra peak enhancement factor introduced in the JONSWAP spectrum, as in the real application all parameters are calculated to approximate the measuring data [14].

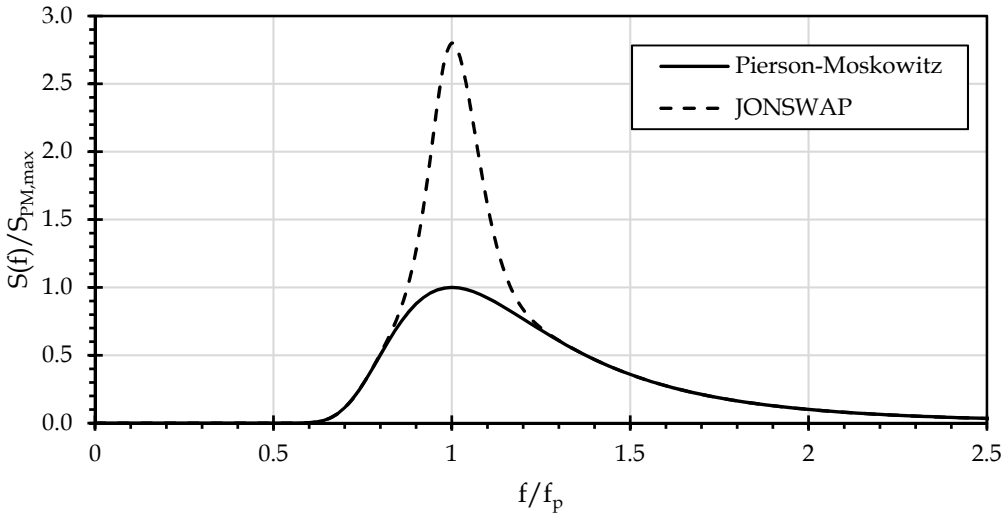

Figure 3. Qualitive comparison of Pierson Moskovitz and JONSWAP spectra.

Sea waves can be classified in different ways, considering the parameters above defined. For example, introducing the ratio $\frac{d_w}{\lambda}$ (water depth divided by wavelength) [21]:

- Shallow water or long wave if $\frac{d_w}{\lambda} < \frac{1}{20}$
- Intermediate water if $\frac{1}{20} < \frac{d_w}{\lambda} < \frac{1}{2}$
- Deep water or short wave $\frac{d_w}{\lambda} > \frac{1}{2}$ Considering the wave period T [14,27], the following definitions are used:
- Capillary waves ($T < 0.1$ s), generated by wind and restored by surface tension
- Ultra-gravity waved (0.1 s $< T <$ 1 s) generated by wind and restored by surface tension and gravity
- Gravity waves (1 s $< T <$ 30 s) generated by wind and restored by gravity
- Infra-gravity waves (30 s $< T <$ 5 min), caused by wind and atmospheric pressure gradients and restored by gravity
- Long-period waves (seiches, storm surges, tsunamis, with a period 5 min $< T <$ 12 h), caused by atmospheric pressure gradients and earthquake and restored by gravity
- Ordinary tidal waves (12 h $< T <$ 24 h), due to the gravitational attraction of celestial bodies (moon and sun) and restored by gravity and Coriolis force
- Trans-tidal waves ($T >$ 24 h), due to storms and gravitational attraction and restored by gravity and Coriolis force.

In oceanography, the term "sea state" is used to indicate the temporary (about a half-hour) and local conditions of the sea surface (with respect to wind waves and swell) as a consequence of wind interaction. The World Meteorological Organization (WMO) defines the sea states according to the Douglas Sea Scale, reported in Table 2.

Table 2. Sea States Codes based on Douglas Sea Scale.

Code	H_s	Characteristics
0	0	Calm (glassy)
1	<0.1	Calm (rippled)
2	0.1–0.5	Smooth (wavelets)
3	0.5–1.25	Slight
4	1.5–2.5	Moderate
5	2.5–4	Rough
6	4–6	Very rough
7	6–9	High
8	9–14	Very high
9	>14	Phenomenal

Analyzing the phenomenon of sea wave propagation, the group velocity v_g is introduced, representing the velocity at which wave-energy travels, and defined by Equation (20):

$$v_g = \frac{d\omega}{dk} \tag{20}$$

In general, the phenomenon is influenced by the water depth. Considering a finite water depth d_w, the wavenumber $k = 2\pi/\lambda$ and the angular frequency $\omega = 2\pi/T$ are related by the dispersion relation, expressed by Equation (21).

$$\omega^2 = gk\ tanh(kd_w) \tag{21}$$

It is interesting to observe that in the case of deep water ($d_w/\lambda > 1/2$), the term $tanh(kd_w)$ is close to 1; in the case of shallow water ($d_w/\lambda < 1/20$) the same term is equivalent to kd_w [24]. Thus, in these cases, Equation (21) is replaced by Equation (22):

$$\omega^2 = \begin{cases} gk & for\ \frac{d_w}{\lambda} > \frac{1}{2} \\ gk^2 d_w & for\ \frac{d_w}{\lambda} < \frac{1}{20} \end{cases} \tag{22}$$

Combining the equations above reported, the velocity group is given by Equation (23) [22]:

$$v_g = \frac{1}{2} v_p \left(1 + \frac{2kd_w}{sinh\ 2kd_w}\right) \tag{23}$$

that can be simplified in two forms, according to the case of shallow water and deep water, respectively (see Equation (24)).

$$v_g = \begin{cases} v_p \ \ for\ \frac{d_w}{\lambda} < \frac{1}{20} \\ \frac{1}{2} v_p \ \ for\ \frac{d_w}{\lambda} > \frac{1}{2} \end{cases} \tag{24}$$

With the target to exploit sea waves as a renewable energy source, it is important to evaluate the amount of energy associate with the phenomenon.

It is possible to define the total amount of energy, related to sea wave for a unitary surface E_t. (sum of kinetic and potential energy) according to Equation (25):

$$E_t = \frac{\rho g}{8} H^2 \tag{25}$$

The value 8 (instead of 2) at the denominator is because wave height is double the wave amplitude.

The wave-energy flux is defined as the power of a unitary wavefront, which is given by Equation (26):

$$\varphi = \frac{\rho g}{8} H^2 v_g \tag{26}$$

Equations (25) and (26) can be applied only for a monochromatic wave spectrum. Since the real sea states are represented by a sum of several monochromatic waves, an approximation is given by Equations (27) and (28), using the definition of significant height.

$$E_t \approx \frac{\rho g}{16} H_s^2 \tag{27}$$

$$\varphi \approx \frac{\rho g}{16} H_s^2 v_g \tag{28}$$

The phase velocity for gravity wave is given by Equation (29):

$$v_p = \frac{\lambda}{T} = \sqrt{\frac{g}{k}} = \sqrt{\frac{g\lambda}{2\pi}} = \frac{gT}{2\pi} \tag{29}$$

consequently, in the case of deep water (where $v_g = v_p/2$), the wave-energy flux is finally obtained, according to Equation (30):

$$\varphi = \frac{\rho g^2}{64\pi} H_s^2 T_e \tag{30}$$

In the literature, this equation is universally adopted to estimate the wave-energy potential in a specific site, knowing the energy period T_e and the significant height H_s [21,22,28,29].

As introduced before, the sea state, identified by the significant height and the energy period, represents one of the several possible conditions that can be observed in the site.

A simple way to report data on the measured sea states is the scatter table (see Figure 4), reporting the equivalent hours in which a specific condition (T_e, H_s) is measured (picture on the left) or the corresponding annual energy availability (picture on the right).

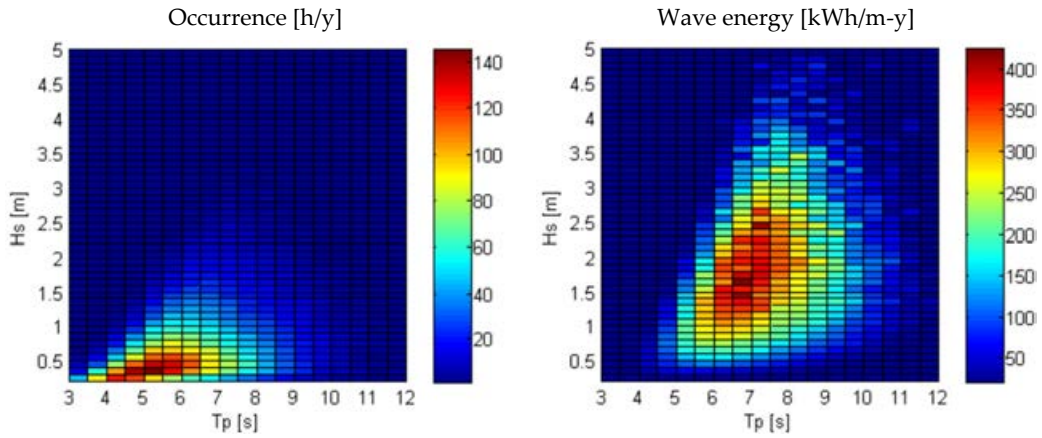

Figure 4. Examples of scatter tables on the island of Pantelleria (Italy) [30].

A generic device to exploit the sea wave-energy source is affected by energy efficiency, due to the transferring of energy from the sea wave to the device (hydraulic efficiency η_{hy}) and the internal transformation to electricity (electrical efficiency η_e). According to the definition of sea wave flux (power per unitary length of wavefront), the electricity production from the sea waves can be estimated by Equation (31):

$$E_{sw} = d_c \sum_{i=1}^{n} \sum_{j=1}^{m} \frac{\rho g^2}{64\pi} H_{s,i}^2 T_{e,j} \eta_{hy}(H_{s,i}, T_{e,j}) \eta_e(H_{s,i}, T_{e,j}) t_{i,j} \quad (31)$$

where d_c is the equivalent diameter of the system that recovers the energy from sea wave, $H_{s,i}$ is the i-th class of significant height, $T_{e,j}$ is the j-th class of energy period and $t_{i,j}$ is the number of hours in which the condition $(H_{s,i}, T_{e,j})$ is measured.

A simplified equation can be also adopted if a monthly average wave-energy flux $\varphi_{m,i}$ is available:

$$E_{sw} = d_c \eta_{hy} \eta_e \sum_{i=1}^{n} \varphi_{m,i} t_i \quad (32)$$

assuming an average hydraulic efficiency η_{hy}, an average electrical efficiency η_e of the system $\eta_{e,w}$, and indicating with h_i the number of hours per month [31].

In the next section, the authors have the aim to list the technologies and the devices developed and installed, reporting on their actual success or failure.

3. State of Art

Among the renewable energy sources, the exploitation of sea waves represents a recent sector, despite the first patent was registered in France in 1799 [32]. Many authors claim that sea waves could play a significant role in the energy sector, especially in small islands [33–35]. Recent statistics indicate that the total theoretical wave-energy potential could achieve 30×10^6 GWh/year; however, this renewable source is irregularly distributed worldwide [36,37]. As shown in Figure 5, there are some hot spots (red-colored areas in the picture), i.e., regions with the highest values of wave-energy potential. The most energetic area is the southern part of Australia, Africa, and America, because of the limited presence of lands. Other relevant areas are located between North America and Japan in the Pacific Ocean and between Europe, Greenland, and North America in the Atlantic Ocean. All these regions are exposed to extreme weather conditions, for this reason, sea wave harvesting is complicated [20,38].

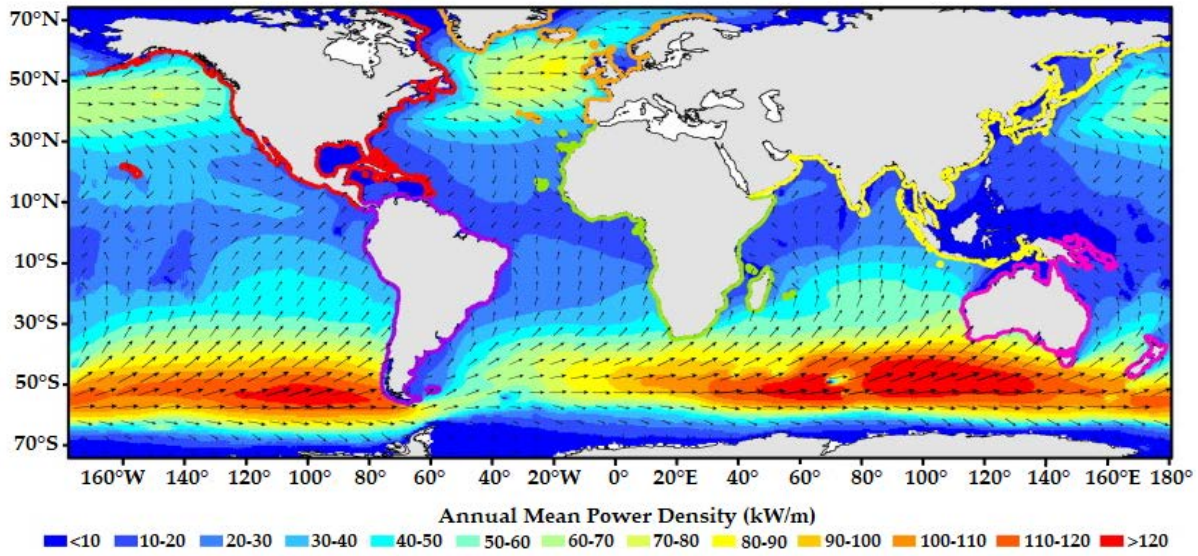

Figure 5. Global wave power GIS map (Reproduced with permission 5139241219046 from [25], Elsevier, 2012).

In this context, the device able to extract energy from sea waves and produce electrical energy or other useful energy output is commonly defined as Wave-Energy Converters (WEC) [32]. These systems are classified using different criteria such as the position to the coastline, the typical size, the orientation to the direction of wave propagation, or the working principle [39]. As shown in Figure 6, considering the orientation of the system to the direction of wave propagation, it is possible to define [40]:

- **Attenuators**, these systems are oriented parallel to the wave direction. Since the device has a length of the same order as the wavelength, it adapts its shape to the wave profile, extracting energy from sea waves.
- **Point absorbers**, these systems work independently of wave direction due to their small sizes in comparison with the wavelength.
- **Terminators**, these systems are oriented perpendicular to the direction of wave propagation. Sea wave ends on the device, transferring its energy.

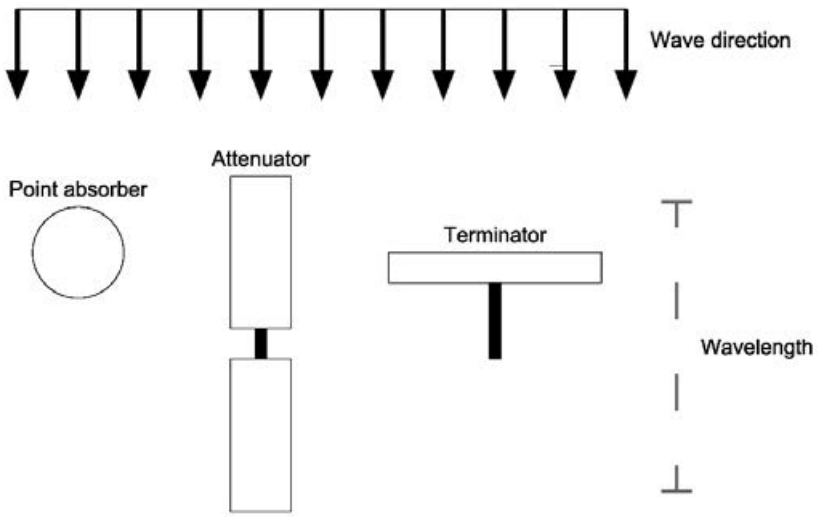

Figure 6. Global wave power GIS map.

Considering the working principle, the following categories are identified [41]:

- **Oscillating water column.** In this system, sea wave enters inside a chamber open to the atmosphere. Inside the chamber, sea wave produces a vertical water oscillation.

The air inside the chamber is pressurized and depressurized by the water oscillation, producing a bidirectional airflow usable to run special wind turbines. The system can be installed on the coastline or integrated into a floating device.

- **Wave-activated bodies**. In this case, the sea wave produces relative motions on the systems, running the energy converters. This kind of system can be assembled in several configurations to produce a rotation or a translation. About the installation, there are floating systems and submerged ones.
- **Overtopping devices**. In this case, seawater is conveyed in a reservoir, using a ramp to convert the kinetic energy of sea waves into potential energy. The water is consequently spilled from the reservoir and used to produce electricity, using a low-head hydro turbine.

About the distance from the coastline, it is common to define the following regions, Figure 7:

- **Onshore**. In this case, the system is directly fixed on the mainland, simplifying the maintenance and the installation of the device.
- **Nearshore.** It represents the transition region between the shoreline and the effective offshore area. In this zone, sea wave energy starts to be dissipated by the seabed. In simple terms, the nearshore region starts where the water depth is about half of the wavelength and ends where the depth is one-twentieth of wavelength.
- **Offshore**, the region where the sea wave phenomenon is practically not influenced by the seabed. In this area, waves are strong and regular.

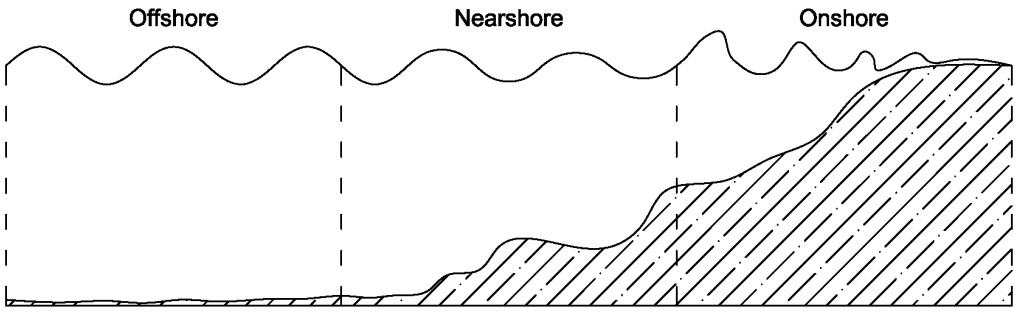

Figure 7. Classification of WEC based on the distance from the coastline.

After this classification, a list of devices, divided into working principles, is reported.

3.1. Oscillating Water Column

Several Oscillating Water Column (OWC) devices have been proposed in the past. According to the position of the system from the coastline, OWC devices can be classified as fixed or floating [37].

In the first case, the OWC plant is installed via a fixed structure on the shoreline or close to it, or in natural or artificial structures, such as breakwaters and rock cliffs [37].

The installation of WEC directly on the shoreline has several benefits. The maintenance operations are simplified, reducing the relative costs. At the same time, the costs for the mooring system are minimized. Furthermore, the entire electrical equipment for the energy conversion is installed out of the water [32].

As mentioned before, the OWC devices are designed to produce a vertical oscillation of water inside a chamber to produce the alternative compression and expansion of the air inside the same chamber. Since the airflow changes continually its direction, the traditional horizontal-axis air turbines cannot be adopted. A solution is represented by the Wells turbine, developed in the mid-1970s by Alan Arthur Wells (in that period professor at Queen's University of Belfast) [32].

The Wells turbine is a low-pressure air turbine, characterized by the ability to rotate in one direction independently of the airflow direction. The blades are characterized by symmetrical airfoils where the plane of the symmetry is the same as the plane of rotation

and perpendicular to the airflow direction. As reported in [32], the Wells turbine is affected by a low (or negative) torque in the case of a small airflow rate; significant aerodynamic losses, and noise in comparison with other wind turbines. Thus, this turbine requires a greater section to achieve the same power output as other turbines. Nevertheless, the Wells turbine has been applied in several OWC plants.

As an example of a full-scale OWC system, the Kværner Brug's OWC plant was realized at Toftesfallen (Norway) in 1985 [42], with an electrical rated power of 500 kW [43]. The lower part was realized in concrete, with a height of 3.5 m above sea level. As reported in Figure 8, this part of the system formed a chamber, communicating to the sea under the water level. The upper part (steel tower), achieving the height of 21 m, was equipped with a self-rectifying air turbine, with a rated power of 500 kW. Unluckily, this plant was destroyed by a severe storm at the end of 1988. Despite the proposal to replace the damaged part, the system was decommissioned, keeping only the concrete part on the testing site. In its short operative life, the Kværner Brug's OWC plant delivered 29 MWh to the electrical grid [44].

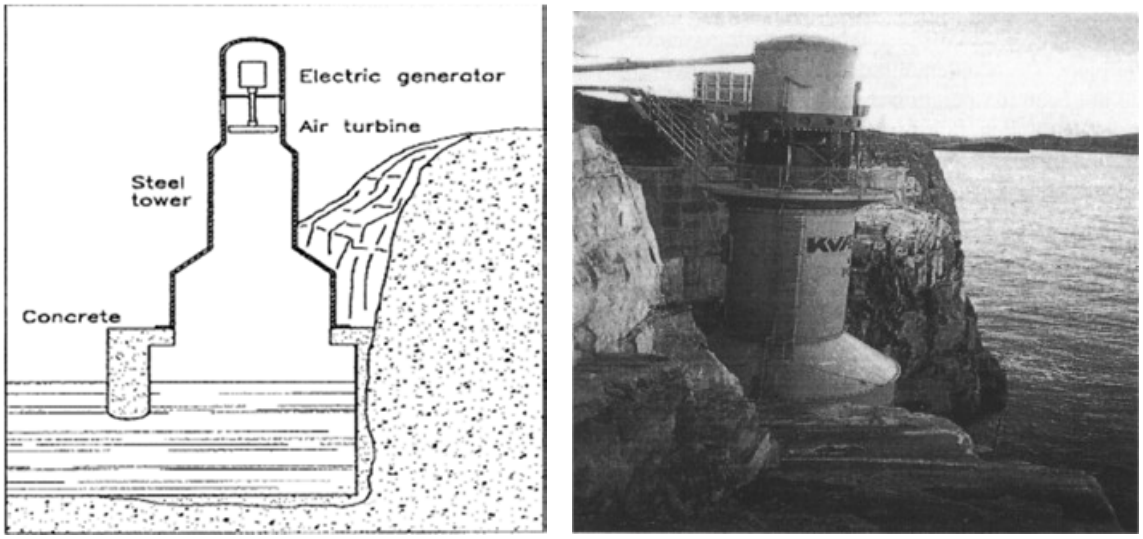

Figure 8. Sectional drawing (left) and view (right) of the Kværner Brug's OWC plant (reproduced with permission 5139250049270 from [42], Elsevier, 2003).

In 1990 an OWC system was installed at Vizhinjam (Trivandrum, Kerala, India), composed by a concrete caisson, and installed near the original breakeven structure. The project considered the installation of a Wells turbine coupled with an induction generator (150 kW) in order to be directly coupled with the electrical grid [45].

In reality, the results were under the expectation: the output power was highly variable in the range 0–60 kW in a few seconds and the induction motor frequently was an electrical load instead of a generator, consuming more energy than the energy produced [46]. The plant was inactive for a long period. In 2004 the plant was investigated to supply a Reverse Osmosis desalination plant. This OWC device was finally decommissioned in 2011 [47]. This OWC system is reported in Figure 9.

Based on the same principle, in 2000 the Islay LIMPET (Land Installed Marine Power Energy Transmitter) was installed on the Scottish island of Islay. This plant was realized and operated by Wavegen in cooperation with the Queen's University of Belfast. Islay LIMPET was the full-scale version of a previous prototype (75 kW) realized in 1991. The OWC system is reported in Figure 10.

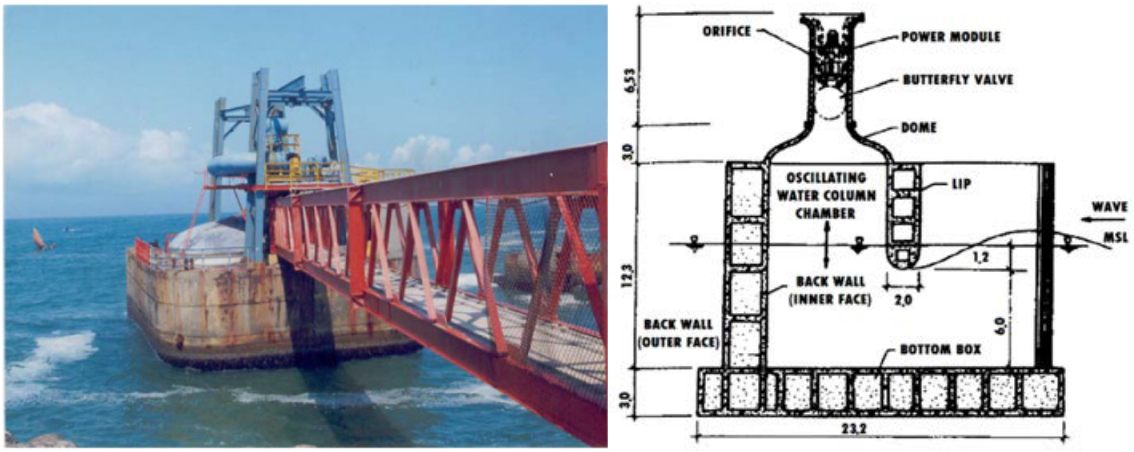

Figure 9. Photo (**left**, reproduced with permission 5152420320606 from [48], Elsevier, 2018) and section view (**right**, adapted with permission 5152420556915, from [49], Elsevier, 1997) of the OWC device at Vizhinjam.

Figure 10. LIMPET OWC plant installed on the island of Islay (Scotland, UK) (Reproduced with permission 5139250512092 from [50], Elsevier, 2016).

The envelope of LIMPET was entirely realized in concrete on the shoreline. It was equipped with two Wells turbines, each one with a rated power of 250 kW [3]. However, the generated power achieved a peak of 180 kW in the first two years of operation, for this reason, the plant was declassed to a rated power of 250 kW [51]. The plant demonstrated the working principle, revealing the issue of noise generation due to the operation of Well turbines. A noise attenuator chamber was added at the end of the turbine chamber, however, causing malfunctioning to the device [50]. The plant was decommissioned in 2012 and today only the concreate building remains on the shoreline.

Similar technology was also developed in Portugal, under the supervision of Instituto Superior Técnico of Lisbon. In 1999 a full-scale (400 kW) OWC plant was realized in Pico Island (Azores, Portugal) [50]. Some problems were due to malfunctions of the Wells turbine and its support. The project was concluded in January 2018, demonstrating the feasibility of this technology [52]. The Pico Plant is reported in Figure 11.

In 2011, an OWC plant was inaugurated in the bay of Mutriku (Spain) [53]. The power plant is 100 m long and has an installed power of 296 kW. It is composed of 16 OWC chambers, each one equipped with a Wells turbine. The producer indicated a total electricity production equal to 2.1 GWh (updated to the end of September 2020) [54]. The OWC system is reported in Figure 12.

An OWC system, called REWEC3 (REsonant Wave-Energy Converter), has been developed in Italy, by the University of Reggio Calabria [37]. This system is designed to be incorporated into a traditional vertical breaker in the harbor. In comparison with other OWC devices, the main difference is the U-shape connection between the internal chamber

and the sea (see Figure 13) that is chosen to adapt the resonance frequency of the system to sea wave. Thus, it is possible to maximize the energy extraction [55]. In the port of Civitavecchia, a full-scale plant has been installed, composed of 136 chambers and a rated power of 2.5 MW [3]. In 2016 the system, with a length of 100 m, produced 500 MWh/y. After the optimization, the designers want to achieve an annual production of 800 MWh/y.

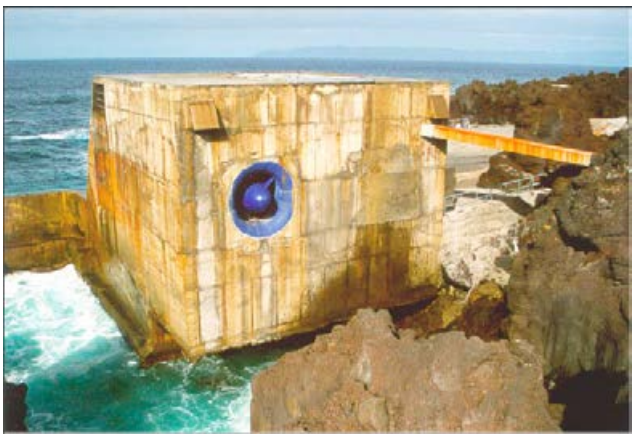

Figure 11. Back view of the OWC plant installed on the island of Pico (Azores, Portugal) (Reproduced with permission 5139250512092 from [50], Elsevier, 2016).

Figure 12. OWC plant installed in the bay of Mutriku (Spain) [54].

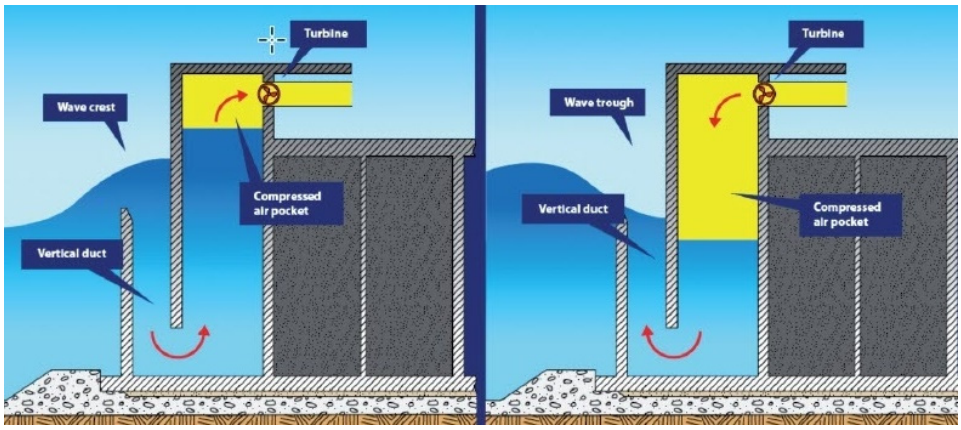

Figure 13. Working principle of REWEC3 [55].

The Yongsoo plant (see Figure 14) is another fixed OWC system that was completed in July 2016 near Jeju Island (Republic of Korea) [3]. The system is installed on the seabed,

at 1.5 km from the coastline [56]. It is equipped with two horizontal-axis impulse turbines, connected to different kinds of generators (a synchronous generator and an induction generator), both with a rated power of 250 kW [3]. The plant has a length of 37 m and a width of 31 m.

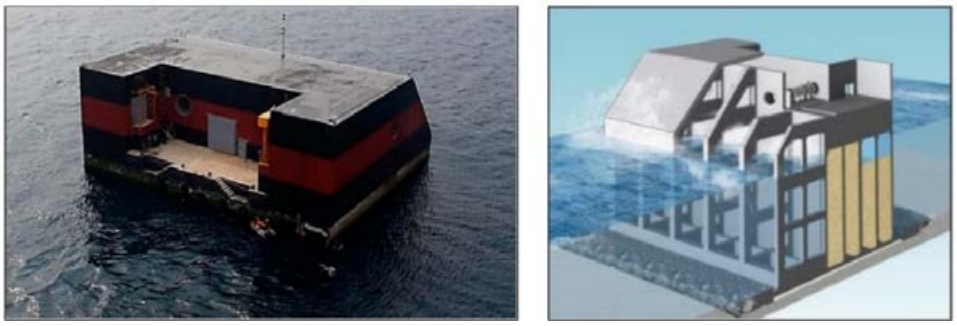

Figure 14. Back (**left**) and perspective views (**right**) of OWC plant at Yongsoo [3].

A similar concept was adopted in King Island, Tasmania. The project was developed by "Wave Swell Energy" company, after a long authorization procedure, including the preliminary evaluation of the energy potential and characteristics of seabed. In 2019, an OWC device (rated power 200 kW) was installed at 100 m from the coastline with a depth of 6 m (see Figure 15 [57]). In January 2021, the device was connected to the electrical grid of Tasmania. According to the project, the device will be removed after a year of testing [58].

Figure 15. Wave Swell (King Island, Australia) [57].

The other family of OWC devices is composed of floating systems. The working principle is the same. The main difference is related to the structure, where the OWC device is installed. Indeed, the most popular solution is represented by the adoption of floating buoys, equipped with chambers used to produce the water oscillation.

One of the first floating OWC was developed in Japan between the 1960s and 1970s by the team of Yoshio Masuda. The system, called Backward Bent-Duct Buoy (BBDB), is composed of a floating buoy, anchored to the seabed and equipped with an L-profiled chamber [59]. This one is open in the back to the sea, under the water level while in the upper part to the atmosphere, through a Wells turbine, as shown in Figure 16 [32,60].

Some years later, other similar systems were developed. Among these, the best known are Sloped Buoy, Spar Buoy, and Mighty Whale reported in Figure 17 [61]. In detail, the Sloped Buoy is composed of three parallel pipes installed on a floating buoy with a tilt angle of 45° [62]. The lower part is open to the sea while the upper part is open to the atmosphere.

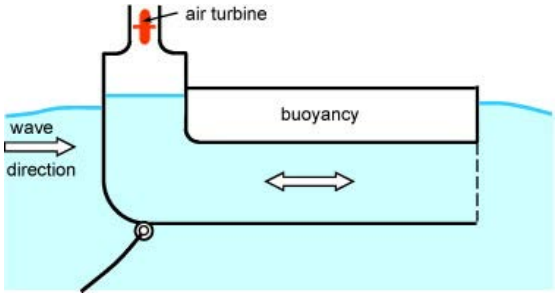

Figure 16. Section of Backward Bent-Duct Buoy (reproduced with license n. 5154830125213 from [32], Elsevier, 2010).

The Spar Buoy is a vertical pipe installed in a floating buoy that has a cylindrical shape. This aspect improves the energy extraction from sea waves because the system works independently of wave direction. For this reason, it is classified as Point Absorber. This device absorbs energy from waves through the heaving oscillation. As consequence, the air inside is alternatively pressurized and depressurized according to the motion [63].

Figure 17. Sloped Buoy (**left**) [61], Spar Buoy (**middle**) [61] and Mighty Whale (**right**) [64].

It is interesting to report the case of Mighty Whale, composed of a buoy with a shape resembling a whale (50 m long and 30 m wide), as shown in Figure 16 [64,65]. This OWC device was composed of two chambers and four Wells turbines, of which two had a rated power of 30 kW, one 10 kW, and one 50 kW (total installed power equal to 120 kW) [66]. The turbines were alternatively activated according to sea states [67]. The prototype was installed 1.5 km away from the coastline of Gokasho Bay (Japan), in July 1998. At the end of 2000, the field test was completed [66]. The device was removed in 2002.

The following Table 3 summarizes the main specifics of the current technologies for sea wave harvesting, based on the OWC principle.

3.2. Wave-Activated Body

The category of Wave-Activated Bodies (WAB) comprises several kinds of solutions for sea wave exploitation. These systems are generally composed of two or more parts, arranged to produce a relative motion and run the energy converter [68].

These systems are generally designed for nearshore or offshore installation, to exploit the more regular waves of the open sea, in comparison with the systems installed on the coastline. However, the installation far away from the coastline increases the number of problems. Indeed, long underwater cables or pipes are required to transfer the energy collected by the WEC to the mainland. These devices need also a mooring system, strong enough to resist extreme weather conditions [69].

Table 3. Summary of the main OWC devices.

Project	Country	Position	Inst.	Power	Status	Note	Ref.
Kværner Brug's OWC	Toftesfallen (Norway)	Fixed Onshore	1985	500 kW	Decommissioned	Damaged by a severe storm in 1988. 29 MWh produced.	[32,42–44]
Vizhinjam OWC	Trivandrum (Kerala, India)	Fixed Nearshore	1990	150 kW	Decommissioned in 2011	Production under the expectation, with high variability. Inactive for a long period.	[45–47]
Limpet	Islay (Scotland, UK)	Fixed Onshore	2000	500 kW	Decommissioned in 2012	High level of noise. The attenuation causes malfunctions.	[50,51]
Pico OWC	Pico Island (Azores, Portugal)	Fixed Onshore	1999	400 kW	The project concluded in 2018	Malfunction due to the Wells turbine and its supports.	[50,52]
Mutriku plant	Mutriku (Spain)	Fixed Onshore (harbor integrated)	2011	296 kW	Operating	Total electrical production 2.1 GWh (end of September 2020)	[53,54]
REWEC3	Civitavecchia (Italy)	Fixed Onshore (harbor integrated)	2016	2.5 MW	Operating	Annual production between 500 and 800 MWh/y	[3,37,55]
Yongsoo plant	Jeju Island (Republic of Korea)	Fixed Offshore (1 km to the coastline)	2016	500 kW	Operating	Adoption of two impulse turbines, connected to different generators	[3,56]
Wave Swell	King Island (Tasmania, Australia)	Fixed Nearshore (100 m to the coastline)	2019	200 kW	Operating	The device will test for a year	[57,58]
Backward Bent-Duct Buoy	Japan	Floating	1960–70	Concept			[32,59,60]
Sloped IPS Buoy	Edinburgh (UK)	Floating	1970–80	Concept			[61,62]
Spar Buoy	Portugal	Floating	2000–15	Concept			[61,63]
Mighty Whale	Gokasho Bay (Japan)	Floating Offshore (1.5 km to the coastline)	1998	120 kW	Decommissioned in 2002		[64–67]

Since there are several WABs, a classification is introduced by considering the working principle of the device as criterium [32]: single-body heaving buoys, two-body heaving systems, fully submerged heaving systems, pitching devices, bottom-hinged systems, and many-body systems.

3.2.1. Single-Body Heaving Buoys

An example is a system composed essentially of a buoy able to move along a metallic strut anchored to the seabed by a universal joint. The idea was the exploitation of this vertical motion to pressurize an air reserve and, consequently, run an air turbine. A prototype, with a buoy one-meter diameter, was tested in 1983 in the Trondheim Fjord (Norway), replacing the air turbine with an orifice [32]. A solution of this technology (Figure 18) was developed at Uppsala University (Sweden), called the Lysekil project [32,70]. As shown in the picture, the vertical motion is used to run a linear generator, with a rated power of 10 kW. This plant was enlarged with the other two WECs and today is currently operating, achieving a total installed power of 30 kW [71].

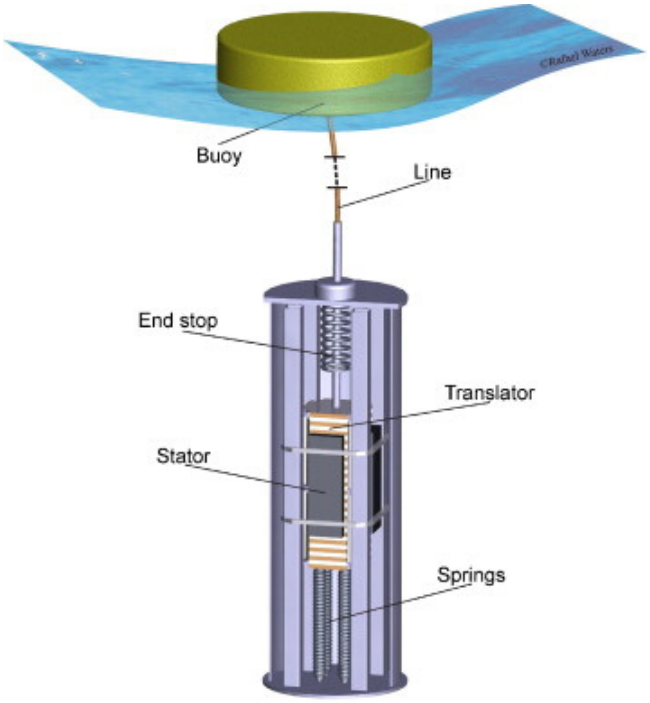

Figure 18. Working principle of Lysekil project (Reproduced with permission 5139260046167 from [32], Elsevier, 2010).

3.2.2. Two-Body Heaving Buoys

The category "two-body heaving systems" was introduced to solve the problem of the distance between the floating buoy and the fixed structure on the seabed, where the energy production occurs. In this case, the WEC is composed of two floating buoys to produce a relative motion usable to extract energy. The shapes of the two floaters are normally different to maximize the relative motion.

As shown in Figure 19, Wavebob is an example of a two-body heaving system. To improve the relative motion between the two parts of the WEC, the central buoy is equipped with a big mass, increasing the inertia, and limiting the vertical motion. The inferior buoy is designed to be submerged at depth enough to minimize the interference with sea waves. The vertical motion produced by the upper buoy (body 1) is used to run an oil pumping system. A small-scale (1:4) prototype was tested in Galway Bay (Ireland) [32,72]. The prototype was installed in 1999 and decommissioned in 2015 because during 2013 the funding ended.

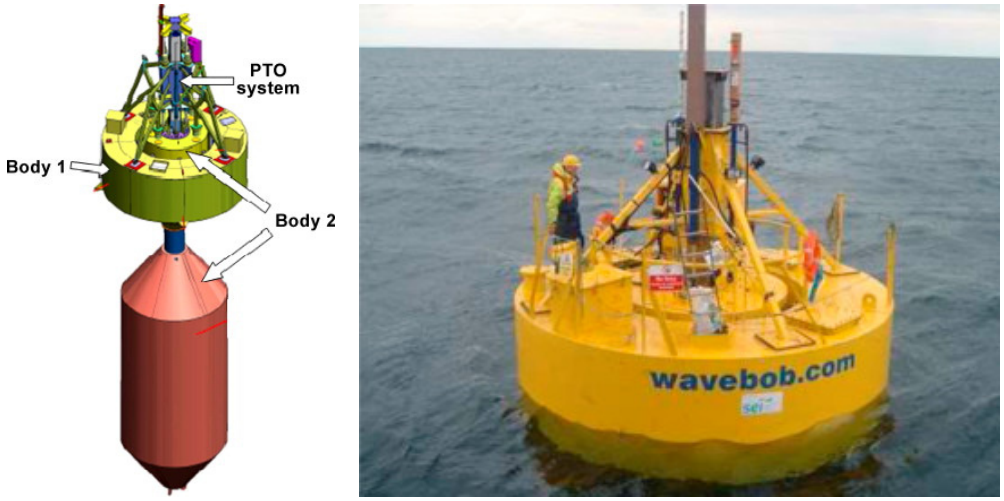

Figure 19. Rendering view (**left**) (Reproduced with permission 5139260046167 from [32], Elsevier, 2010) and external view (**right**) of Wavebob (Reproduced with permission 5139260268553 from [72], Elsevier, 2016).

PowerBuoy is another example of a two-body heaving system, developed by the American company Ocean Power Technologies. As shown in Figure 20 [70,73], this WEC is composed of a floater, which is free to move up and down according to sea wave, and a submerged body, with a disk shape adopted to improve the inertia and hydrodynamic resistance of this part and maximize the relative motion between the two main parts of the device. The idea is the realization of a wave-energy farm, installing several devices, each one producing electricity. To minimize the cost of the electrical connection with the mainland, an offshore substation could be realized. In 2005 a pilot plant (40 kW) was tested in an offshore site, close to Atlantic City (NJ, USA) [70,74]. In 2008, another plant of the same size was installed off the coast of Santoña (Spain) [32].

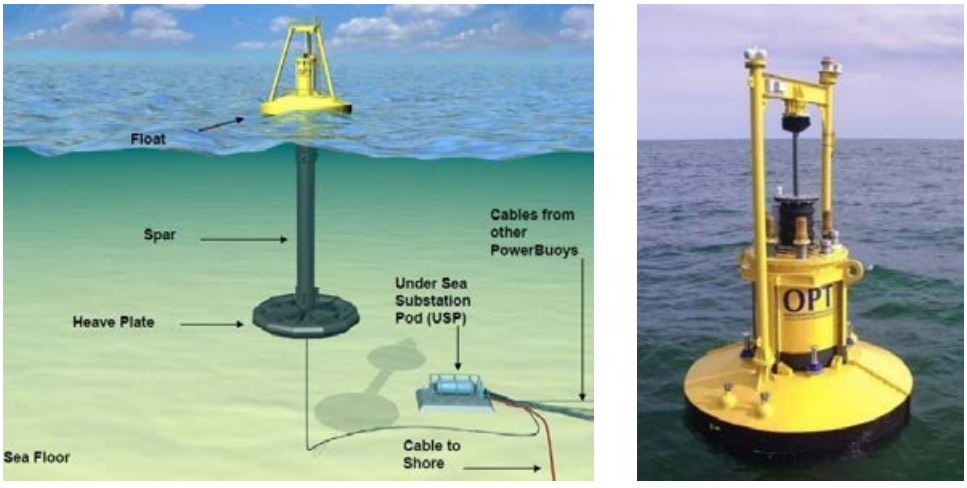

Figure 20. Principle of operation [70] and external view [73] of PowerBuoy.

3.2.3. Fully Submerged Heaving Systems

About the fully submerged heaving systems, an example is the Archimedes Wave Swing, developed in Holland by Teamwork Technology in 1993.

As shown in Figure 21, the system comprises two parts: a basement that is anchored to the seabed, and a floater. The device works using the variation of the hydrostatic pressure applied to the floater that pushes up and down a linear generator installed inside. In 2004,

a pilot plant was tested successfully in Portugal [32]. After this test, AWS Ocean Energy Ltd. was started in Scotland. Recent news reports the development of a 16 kW device [75].

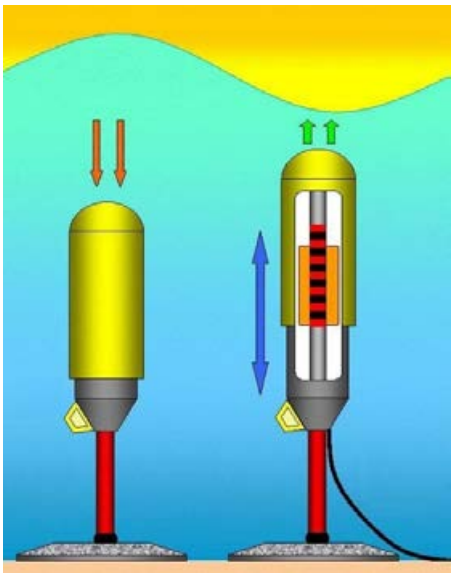

Figure 21. Working principle of Archimedes Wave Swing [76].

CETO (name inspired by a Greek ocean goddess) is another fully submerged device, proposed by Carnegie Clean Energy. This system is designed to be installed in the nearshore, a few meters below sea level. The previous version (CETO 5) was designed to pump water for a station located on the coast where electricity and freshwater are produced, using a Reverse Osmotic unit [77,78]. The project of an upgraded version (called CETO 6, with a rated power of 1.5 MW) was started in Western Australia in 2014 to produce electricity directly on the WEC. The technology is shown in Figure 22. However, the project was discontinued on 31 October 2019 [79].

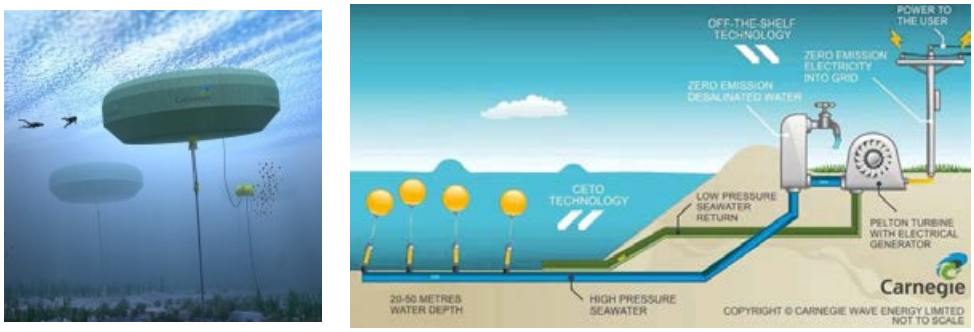

Figure 22. CETO external view [78] and working principle [77].

3.2.4. Pitching Devices

In the pitching devices, the main motion is a relative rotation (usually pitch) among the parts.

A first example was the Salter's Duck (also called the nodding Duck), developed by the team of Prof Stephen Salter at the University of Edinburg (UK), between the 1970s and 1980s. In detail, this device is composed of a floater, with a cam shape (see Figure 23) [80,81]. As a first solution, a hydraulic pumping system was proposed to convert the rotary motion into electricity. As an alternative solution, a gyroscope system was proposed some years later [81].

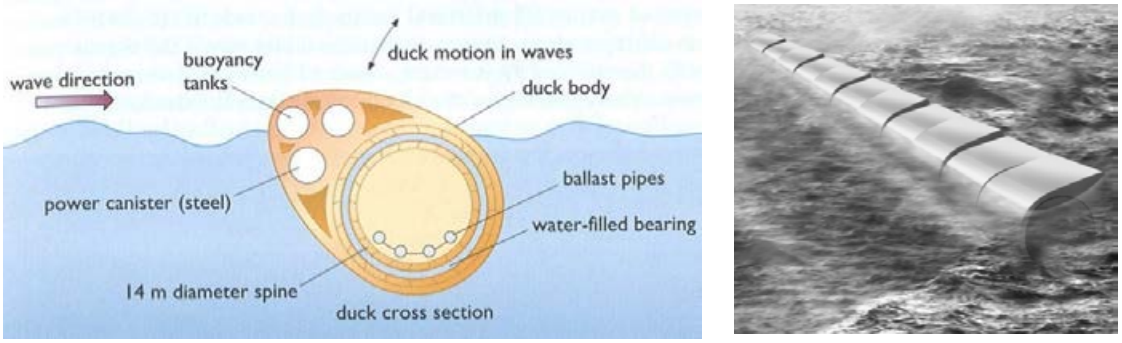

Figure 23. Salter's Nodding Duck. Section (**left**) [81] and rendering view (**right**) (reproduced with license n. 5154830518763 from [80], Elsevier, 2007).

Pelamis was a famous example of a pitching device [32]. It was developed in the UK by Scottish company "Pelamis Wave Power Ltd.". A first prototype, connected to the electrical grid, was tested in Orkney (Scotland) between 2004 and 2007. In 2008 a wave farm with three devices was installed at Aguçadoura (Portugal). Unluckily, the wave farm worked only for two months due to technical failures, causing financial problems to the company. The intellectual property was transferred to the Scottish government in November 2014. This WEC comprised four cylindrical buoys, connected by three Power Conversion Modules (PCM), as depicted in Figure 24 [82–84].

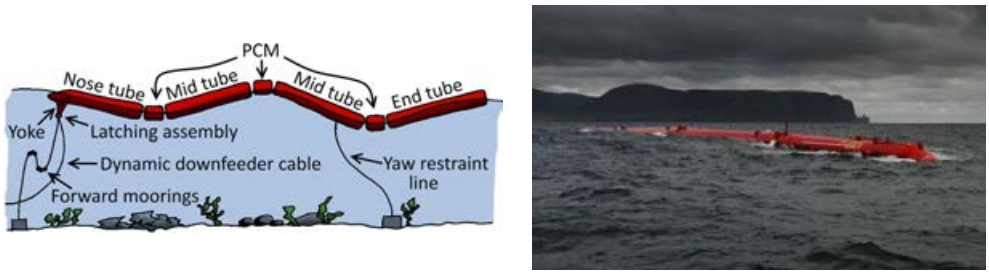

Figure 24. Working principle [82] and external view of Pelamis [83].

In detail, the system had a shape similar to a snake, oriented according to the wave direction, achieving a length of 120 m and a rated power of 750 kW. The working principle of Pelamis was based on the generation of a relative rotation on the PCM, equipped with hinged joints, to pump oil at high pressure into accumulators and then run hydraulic motors coupled with induction generators.

The concept has been recently taken up in other projects, considering the optimization of the geometry of the entire system to maximize the energy harvesting from sea waves [85].

3.2.5. Bottom-Hinged Systems

The Bottom-Hinged Systems are designed to exploit sea waves in shallow water (10–15 m), where the sea motion is mainly horizontal. An example is Oyster, which is illustrated in Figure 25 [86,87].

This device consists essentially of a barrier, made of five cylinders horizontally stacked. Since the barrier is fixed by a horizontal hinge, the braking wave produces a rotation, activating a high-pressure pump. The pressurized water is conveyed along pipes to the coastline, where hydro turbines and alternators are installed to produce electricity. This kind of WEC was proposed by the team of Professor Trevor Whittaker, from the Queen's University of Belfast. The company Aquamarine Power developed and tested two full-scale plants at the European Marine Energy Centre's Billia Croo test site (Orkney): Oyster 1 (315 kW) and Oyster 2 (800 kW). The second version was connected to the grid in 2012 until 2015 when the company ceased trading [88].

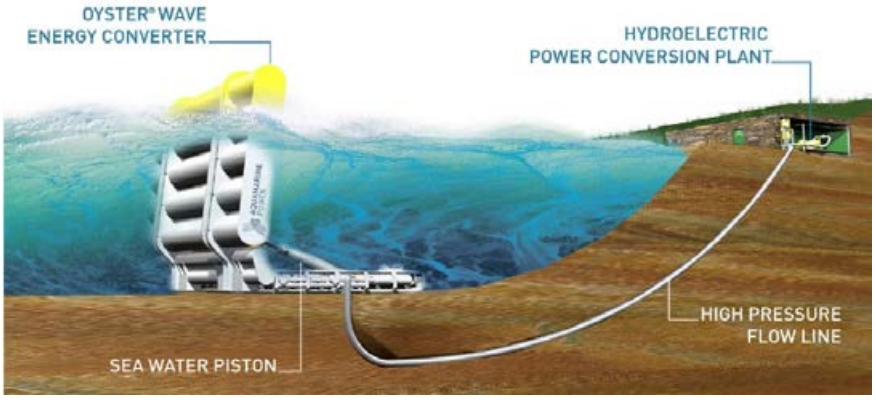

Figure 25. Working principle of Oyster [86,87].

AW energy (a Finnish company) proposed a similar system called Waveroller (see Figure 26) [89]. In 2007, a small-scale (1:4) prototype was tested in Portugal.

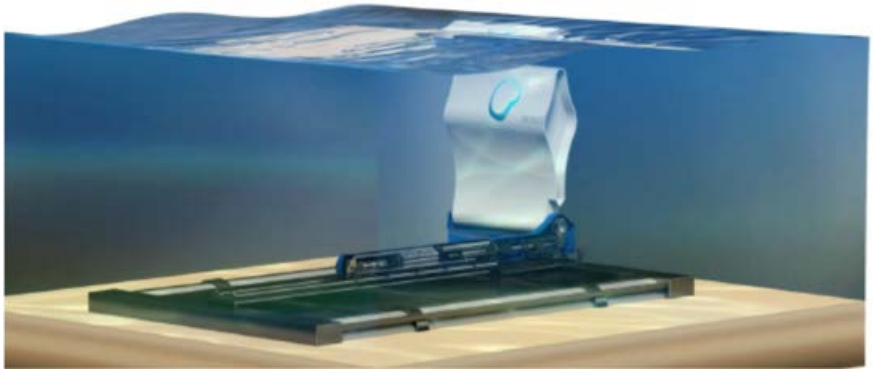

Figure 26. Rendering view of Waveroller [89].

A full-scale prototype was installed in Järvenpää (Finland) in 2015, to optimize the technology. The device is designed to be installed at 0.3–2 km from the shoreline, where the sea depth is between 8 and 20 m. The device has a rated power of 350 kW, equipped with a flap 18 m long and 10 m high [90]. The company is currently working on new projects in Portugal, Mexico, and Southeast Asia [89].

3.2.6. Many-Body System

Wavestar is an example of many-body systems [32]. The first study on this device was started in 2000 by Niels and Keld Hansen in Denmark. A small-scale prototype (1:40) was tested in 2004 at the laboratory of Aalborg University. In 2005, a grid-connected small-scale (1:10) pilot plant was installed at Nissum Bredning. Finally, in 2009 a 1:2 scale prototype was connected to the grid in Hanstholm. The plant was taken down in 2013 [91]. Like other systems described above, Wavestar uses the relative rotation of the buoys to pump oil at high pressure and runs hydraulic motors [32]. The researchers are currently working on the full scale of the device. As shown in Figure 27, Wavestar is composed, is composed by 20 buoys (10 m diameter), arranged in two lines, and able to extract until 6 MW according to the climatic conditions of the North Sea. The system could be also assembled with a star shape, using 60 buoys and achieving a total rated power of 18 MW [91,92].

The same working principle can be applied along the coastline and the breakers of the harbors. An example is the EcoWave System, composed of several floaters, which rise and fall according to the hydrodynamic interaction with sea waves. Using robust arms, the system pressurizes a fluid to run a generator installed on the coastline (see Figure 28 on the left) [93]. In 2016 a wave farm was opened at Gibraltar, located at the southern tip of the

Iberian Peninsula. The plant has currently a rated power of 100 kW but it is planned to achieve 5 MW of installed power [3].

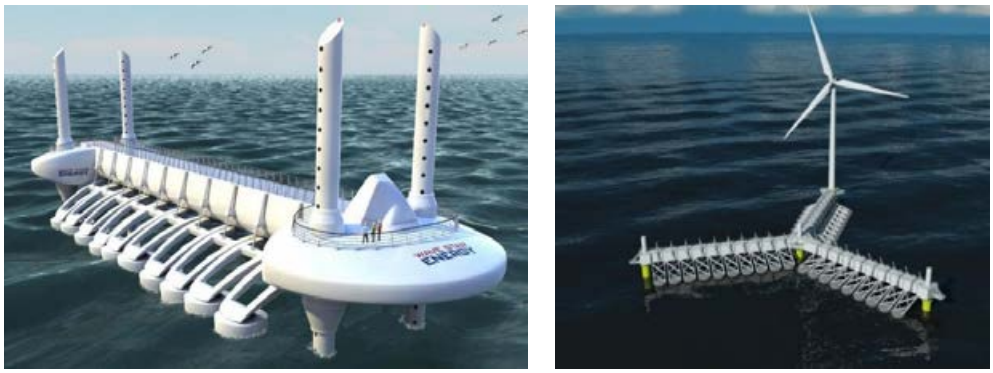

Figure 27. Rendering view of Wavestar [91,92].

Figure 28. View of Eco Wave Systems installed on Gibratal (**left**) [93] and Seahorse power take-off system (**right**) [94].

Based on the same approach, the Seahorse system (50 kW) was installed in 2012 at the Port of Pecem (Brazil) [3,94]. The device was developed by the Federal University of Rio de Janeiro and is composed of two arms, each one equipped with a circular buoy (see Figure 27 on the right) [3,94].

The following Table 4 summarizes the main specifics of the current technologies for sea wave harvesting, based on the WAB principle.

3.3. Overtopping Devices

In the Overtopping Devices (OD), the exploitation of sea waves is based on the conversion of the kinetic energy of water into potential energy, usable by a low-head hydro turbine.

An artificial water reserve should be created at a level superior in comparison to the sea level. To refill the system, a ramp is required to convey sea waves inside the water reserve.

Historically, the first OD pilot plant was the Tapchan (Tapered Channel Wave Power Device), realized at Toftestallen (Norway) in 1985 (see Figure 29) [32,97]. The collector was carved into a rocky cliff, realizing an entrance about 60 m wide and lifting water into a reservoir 3 m above sea level and with a surface of 8500 m^2. To convert the potential energy into electricity, a low-head Kaplan-type hydro turbine was adopted, with a rated power of 350 kW. This plant was damaged by the storm in 1988. The plant was decommissioned in 1991.

Table 4. Summary of the main WAB devices.

Project	Country	Position	Inst.	Power	Status	Note	Ref.
Lysekil Project	Lysekil (Sweden)	Offshore (2 km to the coastline)	2006	30 kW (10 kW each)	Operating	Currently operating and enlarged with 2 WEC (June 2009)	[32,70,71]
Wavebob	Galway Bay (Ireland)	Offshore	1999	Prototype scale 1:4	Decommissioned in 2015	In 2013 end of the funding	[32,72]
Powerbuoy	Atlantic City (New Jersey, USA)	Offshore (22.5 km to the coastline)	2005	Up to 7.5 kW	Operating	Upgrade in 2020 with photovoltaic panels	[32,70,73,74,95]
Archimedes Wave Swing	Portugal	Offshore	2004	Pilot plant	Decommissioned	Available upgrade up to 16 kW	[32,75,76]
CETO 6	Albany, Western Australia	Offshore	2014	1.5 MW	Discontinued	Project discontinued on 31 October 2019	[77–79]
Salter's Nodding Duck	Edinburgh (UK)	Nearshore	1970–1980		Concept		[80,81]
Pelamis P1	Aguçadoura, Portugal	Offshore (5 km to the coastline)	23 September 2008	Three devices (750 kW each) 2.25 MW	Decommissioned November 2008	Worked only for two months due to technical failures on bearings. Financial problems blocked the activities	[32,96]
Oyster 2	EMEC Orkney (UK)	Nearshore	2012	800 kW	Decommissioned	The plant worked until 2015 when the company ceased trading	[86–88]
Waveroller	Järvenpää (Finland)	Nearshore (0.3–2 km from the shore)	2015	350 kW	Project ended	The project ended in October 2013, leaving the device in situ for monitoring	[89,90]
Wavestar	Hanstholm (Denmark)	Nearshore (300 m from the shore)	2009	600 kW	Decommissioned	The plant was taken down in 2013	[32,91,92]
Eco Wave	Gibraltar	Onshore	2016	100 kW	Operating		[3,93]
Seahorse	Pecem (Brazil)	Onshore	2012	50 kW	Operating		[3,94]

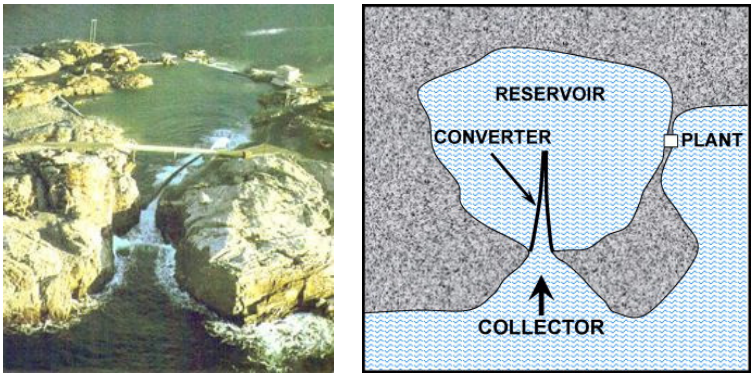

Figure 29. View (**left**) [97] and schematic plan view (**right**) of Tapchan (Reproduced with permission 5139270373963 from [32], Elsevier, 2010).

It is also possible to realize an OD for an offshore application. As an example, the Wave Dragon was a floating slack moored WEC, developed by the Danish company "Wave Dragon Aps". In March 2003 a 20 kW prototype (scale 1:4.5) was installed and tested in the Nissum Bredning fjord until January 2005 [98]. In detail, Wave Dragon is composed of a floating water reserve, refilled with sea waves using two reflectors (see Figure 30) [32,99], and a ramp to convert the kinetic energy into potential energy through the increasing of water level [99]. This kind of energy can be used by Kaplan turbines to run permanent magnets rotary generators. To work properly, the system should be fixed to the seabed by moorings and faced to the wave direction [70].

Figure 30. Views of the small-scale Wave Dragon (**left**) (Reproduced with permission 5139270373963 from [32], Elsevier, 2010) and its working principle (**right**) (Reproduced with permission 5139270591282 from [99], Elsevier, 2009).

The last OD project is called Seawave Slot-Cone Generator, depicted in Figure 31 [3,100]. This system is designed for onshore installation.

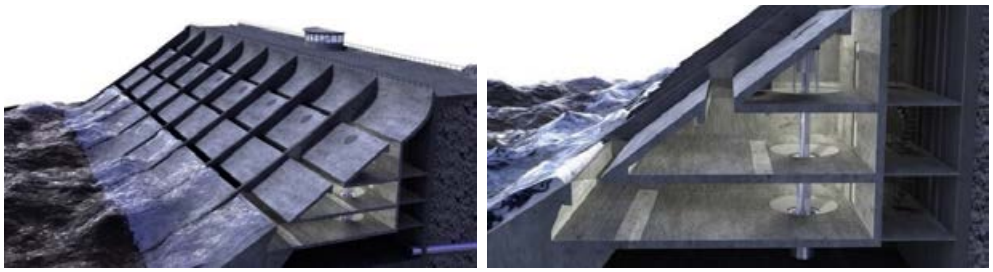

Figure 31. External view (**left**) [3] and section view (**right**) [100] of Slot-Cone.

In detail, the system is composed of three chambers, located at different heights. Each chamber has an opening, located at the superior point. The system has an external

ramp-like shape, to increase the water height and fill the internal chambers. A multistage low-head hydro turbine is used to transform the potential energy of water inside each chamber into electricity. Two pilot plants have been planned for the realization along the west Norwegian coasts, but have not been realized [100].

Finally, OIST Wave-Energy Project can be included in this category. The idea is the conveying of breaking waves inside a duct, to run a low-head hydro turbine. A schematic is reported in Figure 32 [101]. The first test was realized in 2016. After that, 2 half-scale devices (turbine 35 cm wide and rated power of 1.3 kW) were installed and tested at the eastside beach of Kandooma Island in the Maldives in May 2018, accumulating over 7200 h in just ten months (February 2019). Another two full-scale WECs (60 cm turbine, 8 kW peak) were installed in November 2018 (operating over 2000 h in just three months) [101].

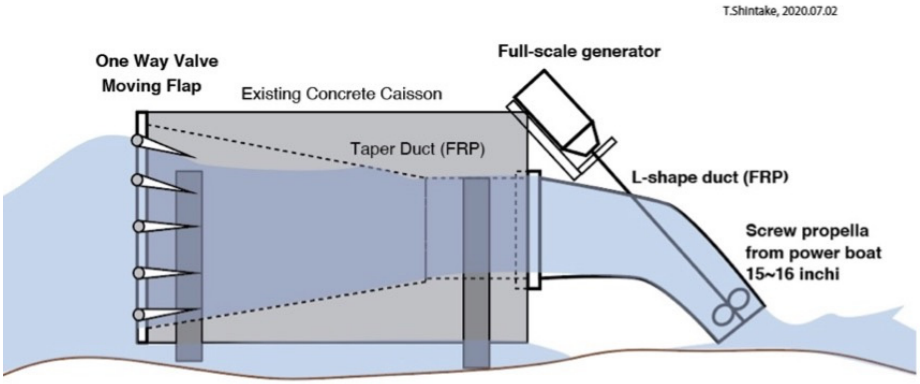

Figure 32. Schematic of the improved design of the Ducted OIST-WEC [101].

The following Table 5 summarizes the main specifics of the current technologies for sea wave harvesting, based on the OD principle.

Table 5. Summary of the main OD devices.

Project	Country	Position	Inst.	Power	Status	Note	Ref.
Tapchan	Toftestallen (Norway)	Onshore (3 m above sea level)	1985	350 kW	Decommissioned in 1991	Damaged by a storm in1988	[32,97]
Wave Dragon	Nissum Bredning (Denmark)	Nearshore	2003	20 kW (scale 1:4.5)	Decommissioned		[32,70,99]
Seawave slot-cone generator	Norway	Onshore			Planned but not realized		[3,100]
OIST-WEC	Kandooma Island (Maldives)	Nearshore	2018	8 kW	Operating		[101]

4. Conclusions

As shown in the lists of various technologies reported in the previous sections, the exploitation of energy from the sea is an area of focus for university studies around the world. Summary tables are provided to bring together all the installations mentioned, showing project name, country of installation/design, technology, year of installation, years of operational life, and notes.

As can be seen, some plants have been successful, producing electricity constantly, and others for various reasons have unfortunately been decommissioned.

Limiting the analysis to the operating wave-energy converter, Figure 33 reports the rated power of the devices, divided by working principle.

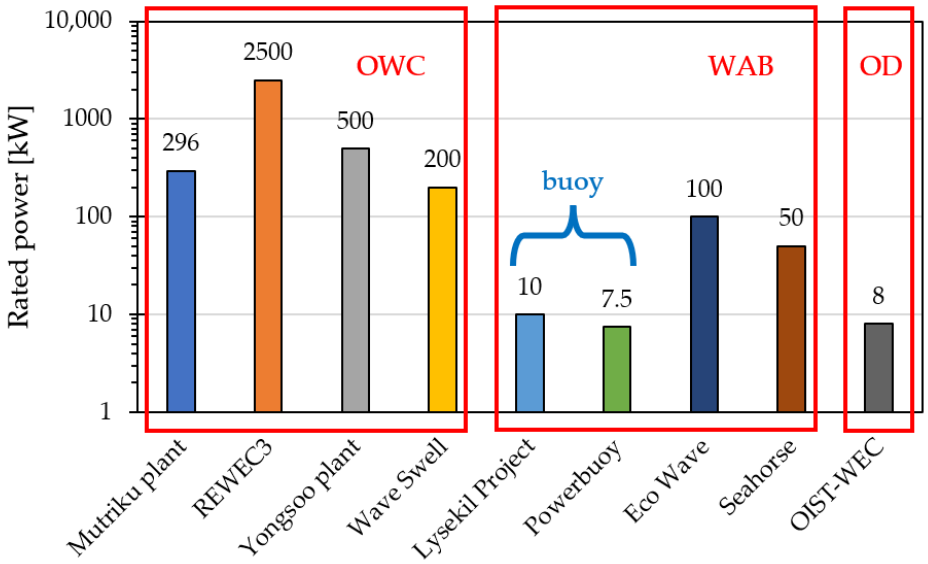

Figure 33. Rated power of the operating wave-energy converter.

It is interesting to observe that the current operating WEC based on the Oscillating Water Column are all integrated on the breakwater. Indeed, this condition minimizes the costs for the installation of the devices because the power plant is close to the electrical grid, and, also, existing infrastructures can be easily converted for this application. The rated power of the existing OWC devices exceeds 200 kW, allowing the production of electrical energy for industrial applications.

About WAB, the current devices can be classified into two categories. The first one comprised floating devices, installed in offshore areas (Lysekil Project and PowerBuoy). In this group, the rated power is about 10 kW, usefully for monitoring and communication in the open sea. The second group comprises devices installed on the breakwaters, such as the OWC devices described above. In this case, the rated power is about 50–100 kW, useful for electrical energy production.

Finally, about the overtopping device, despite the successful tests realized in the past, there is a limited number of projects and proposed devices. The only operating project is OIST-WEC, which is a pilot plant, with a rated power of 8 kW, installable in nearshore areas.

In conclusion, wave-energy harvesting is a very dynamic research area, where different concepts and technologies are currently proposed and developed. Pilot plants and full-scale devices are sometimes tested. However, the number of operating devices is very limited as reported above.

Regardless of the selected technologies, the main barrier is represented by the costs for the development of these systems. The participation of governments becomes very important. Many governments have participated in the construction of energy production plants because it is in their interest to enable the development of renewable technologies, although some not very efficient plants have been decommissioned since funding has been cut off.

In conclusion, it is important to highlight that this energy sector is very is complicated and involves the management of many interrelated factors; for example, in addition to the objective of energy production, attention must be paid to the resistance of the equipment, which must withstand the harsh marine environment. Research has progressed and borne fruit, but it is still possible to aim higher.

Author Contributions: Conceptualization, D.C.; methodology and investigation, D.C. and A.G.; writing—original draft preparation, D.C. and A.G.; writing—review and editing, D.C. and V.F.; supervision, V.F.; project administration, V.F.; funding acquisition, V.F. All authors have read and agreed to the published version of the manuscript.

Funding: This research received no external funding.

Acknowledgments: This work is realized thanks to the technical support of Engosys Enterprise. The research on sea wave harvesting is promoted by the Italian project "Ondaflex" (PO FESR Sicilia 2014/2020), financed by Sicilian Region.

Conflicts of Interest: The authors declare no conflict of interest.

References

1. Saquib Maqsood, M.; Prasad Padhi, B. Ocean Energy: An Insight. In Proceedings of the National Seminar on Sustainable Future, through Leadership & Technology, Bhubaneswar, India, 3–4 March 2017; pp. 59–64.
2. World Energy Council. *World Energy Resources*; World Energy Council: London, UK, 2016; Volume 1.
3. Cascajo, R.; García, E.; Quiles, E.; Correcher, A.; Morant, F. Integration of marine wave energy converters into seaports: A case study in the port of Valencia. *Energies* **2019**, *12*, 787. [CrossRef]
4. Barstow, S.; Mørk, G.; Mollison, D.; Cruz, J. The Wave Energy Resource. In *Ocean Wave Energy*; Springer: Berlin/Heidelberg, Germany, 2008; pp. 93–132. ISBN 978-3-540-74894-6/978-3-540-74895-3.
5. Neill, S.P.; Angeloudis, A.; Robins, P.E.; Walkington, I.; Ward, S.L.; Masters, I.; Lewis, M.J.; Piano, M.; Avdis, A.; Piggott, M.D.; et al. Tidal range energy resource and optimization—Past perspectives and future challenges. *Renew. Energy* **2018**, *127*, 763–778. [CrossRef]
6. Yang, X.; Haas, K.A.; Fritz, H.M. Evaluating the potential for energy extraction from turbines in the gulf stream system. *Renew. Energy* **2014**, *72*, 12–21. [CrossRef]
7. Guo, J.; Zhang, Z.; Xia, C.; Guo, B.; Yuan, Y. Topographic–baroclinic instability and formation of Kuroshio current loop. *Dyn. Atmos. Ocean.* **2018**, *81*, 15–29. [CrossRef]
8. Krug, M.; Schilperoort, D.; Collard, F.; Hansen, M.W.; Rouault, M. Signature of the Agulhas Current in high resolution satellite derived wind fields. *Remote Sens. Environ.* **2018**, *217*, 340–351. [CrossRef]
9. Tinaikar, A. Ocean thermal energy conversion. *Int. J. Energy Power Eng.* **2013**, *2*, 143–146. [CrossRef]
10. World Energy Council. *World Energy Resources: Marine Energy 2016*; World Energy Council: London, UK, 2016; p. 79.
11. Asian Development Bank. *Wave Energy Conversion and Ocean Thermal Energy Conversion Potential in Developing Member Countries*; Asian Development Bank: Mandaluyong City, Philippines, 2014; ISBN 978-92-9254-530-7.
12. Helfer, F.; Lemckert, C.; Anissimov, Y.G. Osmotic power with Pressure Retarded Osmosis: Theory, performance and trends—A review. *J. Memb. Sci.* **2014**, *453*, 337–358. [CrossRef]
13. Curto, D.; Franzitta, V.; Guercio, A. A review of the water desalination technologies. *Appl. Sci.* **2021**, *11*, 670. [CrossRef]
14. Laing, A.; Gemmill, W.; Magnusson, A.; Burroughs, L.; Reistad, M.; Khandekar, M.; Holthuijsen, L.; Ewing, J.; Carter, D. *Guide to Wave Analysis and Forecasting*; World Meteorological Organization: Geneva, Switzerland, 1998; Volume 1998, ISBN 9263127026.
15. Holthuijsen, L.H. *Waves in Oceanic and Coastal Waters*; Cambridge University Press: New York, NY, USA, 2007; ISBN 978-0-511-27021-5.
16. Pecher, A.; Kofoed, J.P. (Eds.) *Handbook of Ocean Wave Energy*; Ocean Engineering & Oceanography; Springer International Publishing: Cham, Switzerland, 2017; Volume 7, ISBN 978-3-319-39888-4.
17. Mackay, E.B.L. Resource Assessment for Wave Energy. In *Comprehensive Renewable Energy*; Elsevier: Amsterdam, The Netherlands, 2012; Volume 8, pp. 11–77. ISBN 9780080878720.
18. Arena, F.; Laface, V.; Malara, G.; Romolo, A.; Viviano, A.; Fiamma, V.; Sannino, G.; Carillo, A. Wave climate analysis for the design of wave energy harvesters in the Mediterranean Sea. *Renew. Energy* **2015**, *77*, 125–141. [CrossRef]
19. Reguero, B.G.; Losada, I.J.; Méndez, F.J. A global wave power resource and its seasonal, interannual and long-term variability. *Appl. Energy* **2015**, *148*, 366–380. [CrossRef]
20. Mork, G.; Barstow, S.; Kabuth, A.; Pontes, M.T. Assessing the Global Wave Energy Potential. In Proceedings of the ASME 2010 29th International Conference on Ocean, Offshore and Arctic Engineering, Shanghai, China, 6–11 June 2010; Volume 3, pp. 447–454.
21. Sierra, J.P.; Mösso, C.; González-Marco, D. Wave energy resource assessment in Menorca (Spain). *Renew. Energy* **2014**, *71*, 51–60. [CrossRef]
22. Cornett, A. A global wave energy resource assessment. In Proceedings of the 18th International Offshore and Polar Engineering Conference, Vancouver, BC, Canada, 6–11 July 2008; ISOPE-2008-TPC-579. pp. 1–9.
23. Sierra, J.P.; Martín, C.; Mösso, C.; Mestres, M.; Jebbad, R. Wave energy potential along the Atlantic coast of Morocco. *Renew. Energy* **2016**, *96*, 20–32. [CrossRef]
24. Krogstad, H.E.; Arntsen, Ø.A. *Linear Wave Theory: Part A: Regular Waves*; Norwegian University of Science and Technology: Trondheim, Norway, 2000.
25. Gunn, K.; Stock-Williams, C. Quantifying the global wave power resource. *Renew. Energy* **2012**, *44*, 296–304. [CrossRef]
26. McCabe, A.P.; Aggidis, G.A. Optimum mean power output of a point-absorber wave energy converter in irregular waves. *Proc. Inst. Mech. Eng. Part A J. Power Energy* **2009**, *223*, 773–781. [CrossRef]
27. Toffoli, A.; Bitner-Gregersen, E.M. Types of Ocean Surface Waves, Wave Classification. *Encycl. Marit. Offshore Eng.* **2017**, 1–8. [CrossRef]

28. Iuppa, C.; Cavallaro, L.; Vicinanza, D.; Foti, E. Investigation of suitable sites for wave energy converters around Sicily (Italy). *Ocean Sci.* **2015**, *11*, 543–557. [CrossRef]
29. Monteforte, M.; Lo Re, C.; Ferreri, G.B.B. Wave energy assessment in Sicily (Italy). *Renew. Energy* **2015**, *78*, 276–287. [CrossRef]
30. Mattiazzo, G.; Giorcelli, E.; Poggi, D.; Sannino, G.; Carillo, A. *Progettazione di un Sistema di Produzione di Energia da Moto Ondoso in Scala Reale*; ENEA: Rome, Italy, 2013.
31. Franzitta, V.; Catrini, P.; Curto, D. Wave Energy Assessment along Sicilian Coastline, Based on DEIM Point Absorber. *Energies* **2017**, *10*, 376. [CrossRef]
32. Falcão, A.F.d.O. Wave energy utilization: A review of the technologies. *Renew. Sustain. Energy Rev.* **2010**, *14*, 899–918. [CrossRef]
33. Rusu, E. Evaluation of the Wave Energy Conversion Efficiency in Various Coastal Environments. *Energies* **2014**, *7*, 4002–4018. [CrossRef]
34. Curto, D.; Neugebauer, S.; Viola, A.; Traverso, M.; Franzitta, V.; Trapanese, M. First Life Cycle Impact Considerations of Two Wave Energy Converters. In Proceedings of the 2018 OCEANS—MTS/IEEE Kobe Techno-Oceans (OTO), Kobe, Japan, 28–31 May 2018; pp. 1–5.
35. Clément, A.; McCullen, P.; Falcão, A.; Fiorentino, A.; Gardner, F.; Hammarlund, K.; Lemonis, G.; Lewis, T.; Nielsen, K.; Petroncini, S.; et al. Wave energy in Europe: Current status and perspectives. *Renew. Sustain. Energy Rev.* **2002**, *6*, 405–431. [CrossRef]
36. Curto, D.; Viola, A.; Franzitta, V.; Trapanese, M.; Cardona, F. A New Solution for Sea Wave Energy Harvesting, the Proposal of an Ironless Linear Generator. *J. Mar. Sci. Eng.* **2020**, *8*, 93. [CrossRef]
37. Aderinto, T.; Li, H. Ocean Wave energy converters: Status and challenges. *Energies* **2018**, *11*, 1250. [CrossRef]
38. Liberti, L.; Carillo, A.; Sannino, G. Wave energy resource assessment in the Mediterranean, the Italian perspective. *Renew. Energy* **2013**, *50*, 938–949. [CrossRef]
39. Wang, L.; Isberg, J.; Tedeschi, E. Review of control strategies for wave energy conversion systems and their validation: The wave-to-wire approach. *Renew. Sustain. Energy Rev.* **2018**, *81*, 366–379. [CrossRef]
40. Curto, D.; Franzitta, V.; Trapanese, M. Designing an innovative system for sea wave utilization. In Proceedings of the OCEANS 2018 MTS/IEEE Charleston, Charleston, SC, USA, 22–25 October 2018; pp. 1–6.
41. Zhao, X.L.; Ning, D.Z.; Zou, Q.P.; Qiao, D.S.; Cai, S.Q. Hybrid floating breakwater-WEC system: A review. *Ocean Eng.* **2019**, *186*, 106126. [CrossRef]
42. Bhattacharyya, R.; McCormick, M.E. Wave Power Activities in Northern Europe. In *Wave Energy Conversion*; Elsevier Science: Amsterdam, The Netherlands, 2003; pp. 95–123.
43. Malmo, O.; Reitan, A. Development of the Kvaerner Multiresonant OWC. In *Hydrodynamics of Ocean Wave-Energy Utilization*; Springer: Berlin/Heidelberg, Germany, 1986; pp. 57–67. ISBN 978-3-642-82668-9.
44. Maurya, A.K.; Singh, S.P. Assessment of Ocean Wave Energy Converters for Indian Coastal Region. *IETE Tech. Rev.* **2020**, *37*, 476–488. [CrossRef]
45. Ravindran, M.; Koola, P.M. Energy from sea waves—The Indian wave energy programme. *Curr. Sci.* **1991**, *60*, 676–680.
46. Khan, J.; Bhuyan, G.S. *Ocean Energy: Global Technology Development Status*; Report prepared by Powertech Labs for the IEA-OES; International Renewable Energy Agency: Abu Dhabi, United Arab Emirates, 2009.
47. Agence Française De Développement; Indian Renewable Energy Development Agency Limited. *Study on Tidal & Waves Energy in India: Survey on the Potential & Proposition of a Roadmap*; AFD: Paris, France; IREDA: New Delhi, India, 2014.
48. Leijon, J.; Boström, C. Freshwater production from the motion of ocean waves—A review. *Desalination* **2018**, *435*, 161–171. [CrossRef]
49. Thiruvenkatasamy, K.; Neelamani, S. On the efficiency of wave energy caissons in array. *Appl. Ocean Res.* **1997**, *19*, 61–72. [CrossRef]
50. Falcão, A.F.O.; Henriques, J.C.C. Oscillating-water-column wave energy converters and air turbines: A review. *Renew. Energy* **2016**, *85*, 1391–1424. [CrossRef]
51. Whittaker, T.J.T.; Beattie, W.; Folley, M.; Boake, C.; Wright, A.; Osterried, M. The Limpet Wave Power Project—The First Years of Operation. *Renew. Energy* **2004**, 1–8.
52. Tethys. Pico Oscillating Water Column. Available online: https://tethys.pnnl.gov/annex-iv-sites/pico-oscillating-water-column (accessed on 30 August 2021).
53. Lacasa, M.C.; Esteban, M.D.; López-Gutiérrez, J.S.; Negro, V.; Zang, Z. Feasibility study of the installation of wave energy converters in existing breakwaters in the north of Spain. *Appl. Sci.* **2019**, *9*, 5225. [CrossRef]
54. Tethys. Mutriku Wave Power Plant. Available online: https://tethys.pnnl.gov/annex-iv-sites/mutriku-wave-power-plant (accessed on 30 August 2021).
55. Mouffe, L.; De Rouck, J.; Verbrugghe, T.; Ranjitkar, G.; Obermann, E.; Wei, P.; Nielsen, K.; Magagna, D.; Soede, M.; De Roeck, Y.-H.; et al. *Annual Report: An Overview of Ocean Energy Activities in 2017*; IEA: Paris, France, 2017.
56. Korea Institute of Ocean Science and Technology KIOST. Yongsoo OWC. Available online: https://openei.org/wiki/PRIMRE/Databases/Technology_Database/Devices/Yongsoo_OWC (accessed on 5 October 2021).
57. Garanovic, A. Wave Swell Energy Deploys UniWave200 off Tasmania. Available online: https://www.offshore-energy.biz/wave-swell-energy-deploys-uniwave200-off-tasmania/ (accessed on 5 October 2021).
58. Wave Swell Energy Ltd. WAVE SWELL. Available online: https://www.waveswell.com/ (accessed on 5 October 2021).

59. Masuda, Y.; Yamazaki, T.; Outa, Y.; McCormick, M. Study of Backward Bent Duct Buoy. In Proceedings of the OCEANS '87, Washington, DC, USA, 28 September–1 October 1987; pp. 384–389.
60. Portillo, J.C.C.; Reis, P.F.; Henriques, J.C.C.; Gato, L.M.C.; Falcão, A.F.O. Backward bent-duct buoy or frontward bent-duct buoy? Review, assessment and optimisation. *Renew. Sustain. Energy Rev.* **2019**, *112*, 353–368. [CrossRef]
61. DTI. *Near Shore Floating Oscillating Wave Column: Prototype Development and Evaluation*; DTI: Makati, Philippines, 2004.
62. Parkin, P.; Payne, G.S.; Taylor, J.R.M. Numerical simulation and tank tests of the free-floating Sloped IPS Buoy. In Proceedings of the 5th European Wave Energy Conference, Cork, Ireland, 17–20 September 2003.
63. Falcão, A.F.O.; Henriques, J.C.C.; Cândido, J.J. Dynamics and optimization of the OWC spar buoy wave energy converter. *Renew. Energy* **2012**, *48*, 369–381. [CrossRef]
64. JAMSTEC. JAMSTEC Gallery. Mighty Whale. Available online: http://www.jamstec.go.jp/gallery/j/research/system/images/system_002_l.jpg (accessed on 6 August 2019).
65. Wu, B.; Chen, T.; Jiang, J.; Li, G.; Zhang, Y.; Ye, Y. Economic assessment of wave power boat based on the performance of "Mighty Whale" and BBDB. *Renew. Sustain. Energy Rev.* **2018**, *81*, 946–953. [CrossRef]
66. OES-Environmental. Mighty Whale. Available online: https://tethys.pnnl.gov/project-sites/mighty-whale (accessed on 6 October 2021).
67. Washio, Y.; Osawa, H.; Ogata, T. The open sea tests of the offshore floating type wave power device "Mighty Whale"—characteristics of wave energy absorption and power generation. In Proceedings of the MTS/IEEE Oceans 2001—An Ocean Odyssey. Conference Proceedings (IEEE Cat. No.01CH37295), Honolulu, HI, USA, 5–8 November 2001; Marine Technology Society: Washington, DC, USA, 2002; Volume 1, pp. 579–585.
68. Vicinanza, D.; Margheritini, L.; Kofoed, J.P.; Buccino, M. The SSG Wave Energy Converter: Performance, Status and Recent Developments. *Energies* **2012**, *5*, 193–226. [CrossRef]
69. Yemm, R.; Pizer, D.; Retzler, C.; Henderson, R. Pelamis: Experience from concept to connection. *Philos. Trans. R. Soc. A Math. Phys. Eng. Sci.* **2012**, *370*, 365–380. [CrossRef]
70. Poullikkas, A. Technology Prospects of Wave Power Systems. *Electron. J. Energy Environ.* **2014**, *2*, 47–69.
71. Leijon, M.; Boström, C.; Danielsson, O.; Gustafsson, S.; Haikonen, K.; Langhamer, O.; Strömstedt, E.; Stålberg, M.; Sundberg, J.; Svensson, O.; et al. Wave energy from the North Sea: Experiences from the lysekil research site. *Surv. Geophys.* **2008**, *29*, 221–240. [CrossRef]
72. Tarrant, K.; Meskell, C. Investigation on parametrically excited motions of point absorbers in regular waves. *Ocean Eng.* **2016**, *111*, 67–81. [CrossRef]
73. Patel, S. Ocean Power Technologies Deploys Commercial PowerBuoy with Energy Storage. Available online: https://www.powermag.com/ocean-power-technologies-deploys-commercial-powerbuoy-energy-storage/ (accessed on 30 August 2021).
74. Globe News Wire. *Ocean Power Technologies Successfully Deploys APB350 PowerBuoy Off the Coast of Atlantic City, New Jersey*; Ocean Power Technologies: Princeton, NJ, USA, 2015.
75. Frangoul, A. In Scotland, Wave Energy Device Reaches Critical Milestone, Gears up for Testing. *CNBC*. Available online: https://www.cnbc.com/2021/06/25/wave-energy-device-reaches-critical-milestone-gears-up-for-testing-.html (accessed on 25 June 2021).
76. Blackledge, J.; Coyle, E.; Kearney, D.; McGuirk, R.; Norton, B. Estimation of wave energy from wind velocity. *Eng. Lett.* **2013**, *21*, 158–170.
77. Alfarsi, H. CETO System: Clean Electricity and Water Desalination Using Ocean Waves. *Profolus*. Available online: https://www.profolus.com/topics/ceto-system-clean-electricity-water-desalination-oceanic-waves/ (accessed on 28 May 2021).
78. Hastie, H. Resurfacing: Collapsed WA wave energy company wants $5m for a rebirth. *The Sydney Morning Herald*. Available online: https://www.smh.com.au/topic/cce-cf (accessed on 17 April 2019).
79. ARENA. Carnegie CETO 6 Technology. Available online: https://arena.gov.au/projects/carnegie-ceto-6-technology/ (accessed on 6 October 2021).
80. Falnes, J. A review of wave-energy extraction. *Mar. Struct.* **2007**, *20*, 185–201. [CrossRef]
81. Salter's Nodding Duck. Available online: https://baonguyen1994.wordpress.com/introduction-to-wave-energy/ocean-wave-technologies/terminators/salters-nodding-duck/ (accessed on 9 August 2019).
82. Thomson, R.C.; Chick, J.P.; Harrison, G.P. An LCA of the Pelamis wave energy converter. *Int. J. Life Cycle Assess.* **2019**, *24*, 51–63. [CrossRef] [PubMed]
83. Wikipedia. Pelamis Wave Energy Converter. Available online: https://en.wikipedia.org/wiki/Pelamis_Wave_Energy_Converter (accessed on 30 August 2021).
84. EMEC. Pelamis. Available online: http://www.emec.org.uk/about-us/wave-clients/pelamis-wave-power/ (accessed on 12 October 2021).
85. Wang, L.G.; Ringwood, J.V. Control-informed ballast and geometric optimisation of a three-body hinge-barge wave energy converter using two-layer optimisation. *Renew. Energy* **2021**, *171*, 1159–1170. [CrossRef]
86. Evans, P. Oyster Ocean Power System to Provide 1 GW by 2020. Available online: https://newatlas.com/oyster-ocean-power-system/11180/ (accessed on 12 October 2021).
87. Poenaru, V.; Scurtu, I.C.; Dumitrache, C.L.; Popa, A. Review of wave energy harvesters. *J. Phys. Conf. Ser.* **2019**, *1297*, 012028. [CrossRef]

88. EMEC. AQUAMARINE POWER. Available online: http://www.emec.org.uk/about-us/wave-clients/aquamarine-power/ (accessed on 12 October 2021).
89. AW Energy. WAVEROLLER. Available online: https://aw-energy.com/waveroller/ (accessed on 30 August 2021).
90. OES-Environmental. SURGE WaveRoller. Available online: https://tethys.pnnl.gov/project-sites/surge-waveroller (accessed on 6 October 2021).
91. Energy Innovation Cluster. WAVESTAR. Available online: https://wavepartnership.dk/wavestar-0 (accessed on 30 August 2021).
92. Jordan Wavestar-002. Available online: https://www.neozone.org/ecologie-planete/wavestar-la-centrale-electrique-qui-utilise-la-houle-pour-produire-de-lenergie/attachment/wavestar-002/ (accessed on 30 August 2021).
93. Eco Wave Power. Photos. Available online: https://www.ecowavepower.com/gallery/photos/ (accessed on 30 August 2021).
94. Zuini, P.; Cepellos, M. Startup usa ondas do mar para gerar energia. *Pequenas Empresas & Grandes Negozios*. 28 July 2015. Available online: https://revistapegn.globo.com/Banco-de-ideias/noticia/2015/07/startup-usa-ondas-do-mar-para-gerar-energia.html (accessed on 2 October 2021).
95. Ocean Power Technologies. PB3 POWERBUOY. Available online: https://oceanpowertechnologies.com/pb3-powerbuoy/ (accessed on 6 October 2021).
96. Kanellos, M. Pelamis Wave Power Jettisons Its CEO, Rough Waters Ahead? *Green Light*. Available online: https://web.archive.org/web/20091003125522/http://www.greentechmedia.com/green-light/post/pelamis-wave-power-jettisons-its-ceo-rough-waters-ahead (accessed on 29 September 2009).
97. Ecthelion. Norwave Wave Power Plant. Available online: https://sketchfab.com/3d-models/norwave-wave-power-plant-482851fc4c8041d99d456289c01dc764 (accessed on 12 October 2021).
98. Bak, P.; Peter, J.; Frigaard, P.; Kofoed, J.P.; Knapp, W.; Department of Civil Engineering Aalborg University; Technical University of Munich. Wave Dragon: Wave power plant using low-head turbines. In Proceedings of the Hidroenergia 04: International Conference and Exhibition on Small Hydropower General, Falkenberg, Sweden, 17–19 June 2004.
99. Tedd, J.; Kofoed, J.P. Measurements of overtopping flow time series on the Wave Dragon, wave energy converter. *Renew. Energy* **2009**, *34*, 711–717. [CrossRef]
100. Buccino, M.; Banfi, D.; Vicinanza, D.; Calabrese, M.; Del Giudice, G.; Carravetta, A. Non breaking wave forces at the front face of Seawave Slotcone Generators. *Energies* **2012**, *5*, 4779–4803. [CrossRef]
101. Shintake, T. OIST Wave Energy Project. Available online: https://groups.oist.jp/qwmu/oist-wave-energy-project (accessed on 2 October 2021).